

Research On Energy Saving and Performance Enhancement of High-End Hydraulic Press With Controllable Accumulator

Lin Hua

Wuhan University of Technology - Mafangshan Campus: Wuhan University of Technology

Zhicheng Xu (✉ 1184492640@qq.com)

Wuhan University of Technology <https://orcid.org/0000-0002-6321-591X>

Yanxiong Liu

Wuhan University of technology

Xinhao Zhao

Wuhan University of technology

Original Article

Keywords: High-end hydraulic press, Energy saving, Hydraulic system, High working performance

Posted Date: January 29th, 2021

DOI: <https://doi.org/10.21203/rs.3.rs-155423/v1>

License:  This work is licensed under a Creative Commons Attribution 4.0 International License.

[Read Full License](#)

1 **Research on energy saving and performance**
2 **enhancement of high-end hydraulic press with**
3 **controllable accumulator**

4 Lin Hua^{1, 2#}, Zhicheng Xu^{1 2, 4**}, Yanxiong Liu^{1, 2*}, Xinhao Zhao^{1, 3}

5 Abstract: Hydraulic fineblanking press is a kind of high-end hydraulic metal forming devices and
6 widely applied in automotive and appliance industry. However, it suffers from the defeat of high energy
7 consumption low energy efficiency. To solve the problem, this study proposed a power-matching
8 strategy by using a novel controllable accumulator which can control the precharge pressure, output
9 flow with high precision. Firstly, the energy characteristics and working performance requirements of
10 the large-sized fineblanking press in a working cycle were investigated. Then, the energy consumption
11 mathematic model coupling with the controllable accumulator was built for designing the key
12 parameters of the accumulators. Based on the load characteristic and the energy model, a controlling
13 strategy of the controllable accumulator was proposed to reduce the imbalance degree of the supplied
14 and demanded power and improve working performance by designing working route of the
15 controllable accumulator. Finally, a detailed hydraulic schematic was designed and applied on the 1000
16 ton hydraulic fineblanking press, which was validated with simulation model. The results show that
17 compared to the traditional system, the energy efficiency of the novel system is improved by 20.35%
18 with lowering the input energy by 169.4 kJ. Besides, the vibration magnitude of the slide block is
19 decreased a lot and the working production efficiency is improved by 10% compared to the traditional
20 system.

The authors Lin Hua and Zhicheng Xu contributed equally to this work.

* Corresponding author. xuzhicheng@whut.edu.cn (Zhicheng Xu), yxliu@whut.edu.cn (Yanxiong Liu)

21 **Keywords:** High-end hydraulic press; Energy saving; Hydraulic system; High working performance

| Nomenclature | | | |
|----------------------|---|--------------|---|
| Abbreviations | | | |
| FC | Fast-closing stage | p_n | Motor nominal power (W) |
| AD | Anomaly detection stage | l | Pipe length (mm) |
| FB | Fineblanking stage | p_s | Overflow pressure |
| UP | Pressure unloading stage | p_u | SAM output power (W) |
| FO | Fast-opening stage | T_{out} | Pump output torque (Nm) |
| PID | Proportion integration differentiation | T_{fic} | Pump internal friction torque (Nm) |
| Symbols | | v_t | Oil velocity in pipe (m/s) |
| A_j | Contact area between the piston and the cylinder block (mm ²) | x_0 | Spool displacement (mm) |
| c | Flow coefficient of cartridges valves (Null) | p_u | SAM output power (W) |
| C_{ic} | Internal leakage coefficient of the cylinder (W/bar ²) | $L1$ | FC stroke |
| C_s | Pump leakage flow rate (Null) | $L2$ | AD stroke |
| d_c | Valves spool diameter (mm) | $L3$ | Whole stroke |
| B_c | Friction coefficient (N/m ²) | x1 | Target signal |
| k_1, k_2 | Constant value parameters of motor (Null) | Greek | |
| q_d | Overflow flow (m ³ /s) | η_v | Pump volumetric efficiency (Null) |
| l | Pipe length (mm) | η_m | Pump mechanical efficiency (Null) |
| n_p | Pump rotational speed (r/min) | μ | Dynamic viscosity of the oil (Ns/m ²) |
| P_a | Valves input pressure (Pa) | ρ | Oil density (kg/m ³) |
| P_b | Valves output pressure (Pa) | α | Valves spool cone angle(°) |
| p_e | Motor power loss (W) | λ | Resistance coefficient along the pipe (Null) |
| p_f | Pipe local loss (W) | Δq | Pump leakage flow (m ³ /s) |
| p_j | Power loss along in parallel pipe (W) | | |

22

23 **1. Introduction**

24 With the increasing of the energy shortage and the worsening of the natural environment, the
 25 energy conservation and the emission reduction concept has been attracted more and more attention all
 26 around the world, which is also an effective way to relieve these problems. On the other hands, with the
 27 fast development of the industrial manufacturing, the CO₂ emission was increased rapidly, which has

28 caused the sea level rise and the extreme climate in recent years. To deal with these serious problems,
29 many international organizations and countries have worked together and assigned some policy of
30 emissions reduction, such as Paris assignment. It is reported that about 31% of total electricity were
31 consumed by the industrial activity in 2012 in the U.S ^[3], of which the manufacturing industry
32 accounted for 90% . Hence, the manufacturing industry is a huge CO2 emissions source caused by the
33 usage of machine tool and press . For these equipment, the most common used method of power
34 transmission is the hydraulic system, especially for these machine with large power, because of high
35 power ratio, long-life, high reliability, convenient stepless speed regulating, auto-control and flexible
36 transmission direction. Actually, most of high power machines take hydraulic transmission as the main
37 driven system with no alternative in present technology. However, the low energy efficiency of
38 hydraulic driven system is also a serious problem, especially in the state of global energy shortage and
39 increased greenhouse effect, which is getting more and more prominent.

40 In the metal forming filed, the hydraulic fineblanking press is the top class because of highest
41 manufacturing precision and production efficiency. The working capacity of the hydraulic fineblanking
42 press can achieve 1000 ton with 30~80 pieces per minute, which requires the demanding working
43 performance of the hydraulic system and bigger installed power compared to the ordinary press ^[6].
44 However, the hydraulic fineblanking press suffers from the same drawbacks with the ordinary press -
45 low energy efficiency only 10% and causes great energy wasted. From the aspect of functions, the
46 forming equipment can be divided into several parts: controller, main hydraulic transmission system,
47 mold and cooling system. Most of energy about 90% of the total input energy is consumed by the
48 hydraulic transmission system. Hence, there is great potential in improving the energy utilization
49 efficiency of hydraulic system ^[7].

50 A high-accuracy energy consumption model is the basis of analyzing energy distribution, which
51 is helpful to better explore the root of low energy efficiency of hydraulic system. From the point of the
52 components level, the energy consumption calculation model of the motor-pump units was built by
53 considering the input and output power, which was able to calculate the static and dynamic properties
54 of the hydraulic system . Furthermore, a more detailed energy consumption model was provided for
55 calculating the power loss of each hydraulic element involving the motor, pump, pipe, valve and so on,
56 which showed a high accuracy . From the aspect of the energy forms, the energy conversion forms of
57 the whole hydraulic system was divided into six parts which comprised electric-mechanical energy,
58 mechanical-hydraulic energy, hydraulic-hydraulic energy, hydraulic-mechanical energy,
59 mechanical-deformation energy, thermal-thermal energy with corresponding impact factors ^[10].
60 However, this model is not easy to use impractically because of too many unknown parameters to be
61 tested in advance. Summarily, the authors Xu and Zhao both indicated that the great energy loss and
62 low energy efficiency mainly resulted from the imbalance of the supplied and the provided energy.

63 To date, many researches have been carried out for improving the energy efficiency,
64 concentrating on three aspects: system structure optimization, high efficiency components and energy
65 management strategies. Intrinsically, all these methods are trying to reduce the energy gap between the
66 supplied and the provided energy.

67 Initially, the structure of hydraulic system is very simple with simple function. With the
68 increasing requirements of the machine, more and more novel functions were developed and added in
69 the hydraulic system such as pressure reduction and flow controlling functions, most of which aimed at
70 improving the working performance rather than energy efficiency in early years. To improve the energy
71 efficiency, a novel closed-loop hydrostatic transmission (HST) system with two hydraulic accumulators

72 was proposed to recover the kinetic energy without any reversion of the fluid flow based on the
73 adaptive fuzzy sliding mode control strategies . This new system saved 10% to 20% more energy than
74 that of the traditional HST system . An energy-saving fast forging system schematic of two-stage
75 pressure source was presented to match the load of different actuators, tested on the 0.6 MN hydraulic
76 forging press platform . In addition, the variable-frequency pump with accumulator, aiming at
77 controlling the output pressure of the pump, was integrated to achieve zero overflow loss through
78 applying fuzzy self-turning closed-loop control strategy, which gained the total energy consumption
79 reduction by 65.3% . The single drive system was separated into several drive subsystems shared by
80 several presses to shorten the waiting time by optimizing the processing schedule ^[15]. Results showed
81 that the energy efficiency of a single hydraulic press in the group is increased by approximately 20%
82 and the average energy consumption can be reduced by 43% compared with the traditional device.
83 Furthermore, a novel energy-efficient system that created a sharing circuit is proposed to connect two
84 actuators by pipes and valves, which could synchronize the falling procedure of one cylinder with the
85 returning procedure of the other. Compared to the undergoes services, this new structure can reduced
86 the energy consumption by 20.61% . A new hydraulic regulation method on district heating system
87 with distributed variable-speed pumps was presented to achieve on-site hydraulic balance for the
88 district heating systems and the energy saving ratio of the district system was 36.1–90.3% less than that
89 of the conventional central circulating pump configuration . To improve the energy efficiency, a
90 combined valve-pump combined with multiple accumulators was presented to match the load profile of
91 fineblanking process . The authors Joshua D and Andrea used the variable displacement with the
92 pressure regulation valves to achieve loading sensing function on excavator, which can match the load
93 well and reduce the overflow loss in idle stage. To reduce the product cost of power unit, a

94 speed-controlled induction motor in combination with a constant-displacement pump was applied in a
95 load-sensing control strategy and gained a good energy-saving effect ^[21]. A displacement variable pump
96 driven by a speed variable electric motor as power source was proposed integrated with a matching
97 method based on the segmented speed and continuous displacement control of the pump, and the
98 energy saving ratio under partial load condition can be up to 33% . There are also other different
99 functions valves integrated on the variable pump to achieve negative-flow control circuit, positive-flow
100 control circuit, and constant power control circuit and so on. These variable pumps with certain
101 functions can save energy to some certain.

102 Another effective way to reduce energy consumption and improve energy efficiency is to
103 recovery the waste energy . This way can make up the gap between the supplied and the demanded
104 energy although the supplied energy cannot match the load profile well. In most case, the energy
105 storage device absorbs the extra energy such as the potential energy of heavy motion part, overflow
106 energy of machining idle time from the power unit, the mechanical energy of rotation part while
107 slowing down . Considering the types of the energy storage device in hydraulic system, the most
108 common used is the hydraulic accumulator because it can be easily integrated into the hydraulic system.
109 The most important thing is no secondary conversion of different energy types for ensuring few energy
110 loss in the energy storage and releasing process while using hydraulic accumulator, which is superior to
111 the chemical battery in which the hydraulic energy should be converted into the kinetic energy of the
112 generator rotor firstly and then converted into electricity by the electro-magnetic induction principle
113 with low conversion efficiency.

114 Equipped with the hydraulic accumulator, many energy regeneration circuit and systems are
115 developed. In construction machine , an energy alternate recovery and utilization system based multiple

116 hydraulic cylinders and hydraulic accumulator was proposed to recovery the potential energy of the
117 bucket, the stick and the boom, which gained comprehensive energy-saving rate is 41.6% compared
118 with the original system . a gravitational potential energy recovery circuit with an energy conversion
119 cylinder and a hydraulic accumulator was proposed ^[28]and these recovery energy can be reused directly
120 without increasing the cost and install power of the machine largely. A valve–motor–generator and a
121 hydraulic accumulator was used for a hybrid hydraulic excavator to recovery the potential energy and
122 got the total energy efficiency of 58% ^[29]. A two-level idle speed control system comprised three stages
123 of idle speed control with a hydraulic accumulator were invented . By optimizing the key parameters,
124 the energy saving efficiency was approximately 36.06%. In addition, the hydraulic accumulator is also
125 applied on the automobile for recovering the braking energy. A new braking pressure coordinated
126 control system was proposed to regenerate the braking energy with three hydraulic accumulators and
127 the braking energy recovery rate reached 47-66% ^[31]. A hybrid power system, involving the hydraulic
128 power unit was proposed and the accumulator was applied to regulate the power relationship between
129 this two power supply units, to save fuel consumption by up to 11%. A regenerative hydraulic shock
130 absorber system was proposed ^[33], which converts the oscillatory motion of a vehicle suspension into
131 unidirectional rotary motion of a generator and improved the energy efficiency by 40%. In addition, the
132 hydraulic accumulator is also widely applied on the wave energy recovery field , which functions as
133 storing energy and pressure stability to improve the energy conversion efficiency.

134 Although the hydraulic accumulator is widely used in various fields like construction machinery,
135 wave energy capturing and automobile, there still exists some drawbacks such as the limited capacity
136 and uncontrollability resulted from the coupling of the output pressure and flow. To increase the energy
137 storage capacity, the utilization efficiency of accumulator with and without elastomeric foam was

138 investigated and the result showed the accumulator had a constant efficiency of about 95% with fully
139 filled with foam . A double-bladder accumulator with filled metallic filler was invented to maintain the
140 isothermy of the gas, which can improve the energy capacity and the dynamic performance . However,
141 the manufacturing process of this kind of accumulator is complex with high cost. A novel hydraulic
142 accumulator that used a piston with an area that varies with stroke to maintain a constant hydraulic
143 system pressure was presented . The results showed that about 16% improvement of energy density
144 was obtained over a conventional accumulator a and the maximum energy density of this novel
145 accumulator was improved to 2.7:1 from 1.8:1. The mechanical flywheel and the hydraulic
146 accumulator was combined to increase the energy storage density, which was applied in the lift system.
147 The analysis results indicated that this novel accumulator maybe solve the problem of the coupling
148 between the pressure and the flow . Although abovementioned methods are potential to improve the
149 energy capacity of the accumulator, few researches are focused on the working performance and the
150 controllability of hydraulic accumulator.

151 Although many advanced energy-saving systems have been developed and much works have
152 been carried out on the hydraulic accumulator for improving the energy capacity, there still lacks of a
153 comprehensive research about the application of hydraulic accumulator on this advanced hydraulic
154 system to achieve high work performance and excellent energy saving effect at the same time. To
155 further improve the overall performance of the fineblanking press, this study proposed a double stage
156 pressure hydraulic system with a novel controllable accumulator with the ability for solving the
157 coupling problem between the output pressure and flow. This novel system can make full use of the
158 hydraulic controllable accumulator with four working modes to eliminate the imbalance of the
159 demanded and the supplied energy with improving the working performance of the fineblanking

160 processing. This study also provided an alternative high-end hydraulic system with high energy
161 efficiency for the metal forming filed. To validate the feasibility of this novel system, a simulation
162 reearch of 1000 ton hydraulic fineblanking press was built to analyze the working performance and
163 energy distribution characteristic.

164 This paper is organized as follows: Section 2 presents the working principle of hydraulic system
165 as well as the novel accumulator; Section 3 establishes energy consumption models of the whole
166 system; Section 4 calculates the key parameters of the accumulator; Section 5 designs the detailed
167 hydraulic schematic of the 1000 ton hydraulic fineblanking press and builds the simulation model of
168 the whole ; Section 6 analyses the working performance and the energy dissipation of this novel system;
169 section 7 gets the conclusions.

170

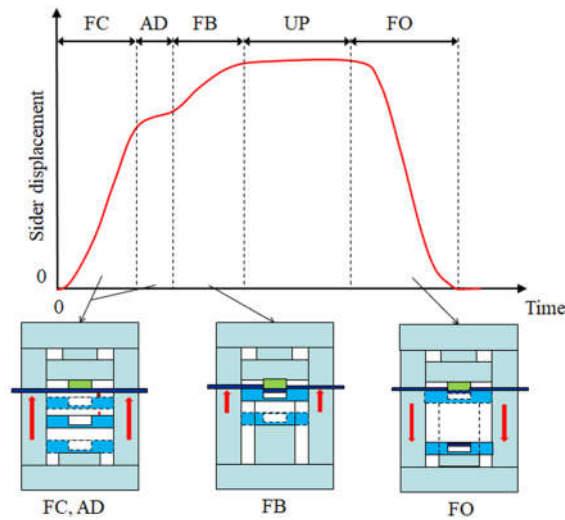
171 **2. System configuration**

172 It is acknowledged that the hydraulic system should serve as the requirement of the metal forming
173 process. This study takes the hydraulic fineblanking press as the case study. Hence, the working
174 principle of fineblanking processing is firstly introduced, which generates the demanding requirements
175 for the hydraulic system.

176 *2.1 Fineblanking processing*

177 Finblanking processing is similar with the stamping processing. The difference between them is
178 that the finblanking processing is near net-shape sheet-metal forming process with higher dimensional
179 accuracy and better surface-cutting quality. In addition, the production efficiency of fineblanking
180 processing can achieve 30-80 pieces per minute, which is almost 7 times higher than that of the
181 stamping processing. From the aspect of working process, the whole fineblanking processing can be

182 divided into five stages as shown in Fig.1: Fast-closing stage (FC), anomaly detection stage (AD),
183 fineblanking stage (FB), pressure unloading stage (UP), and fast-opening stage (FO).



184

185 Fig. 1. The schedule of work processing and the movement of slider.

186 During the FC stage, the lower slider is driven by the hydraulic cylinder to move up. The die is
187 installed on the lower slider and the punch is installed on the upper slide block. Hence, the function of
188 this stage is closing the mould rapidly to prepare for the fineblanking the sheet metal. Because of the
189 long stroke of this stage, to reduce the time interval, the movement speed of the slider should reach
190 80~120 mm/s for high production efficiency, which requires the hydraulic system to be able to provide
191 large oil flow.

192 Due to the expensive price of the mould and to prevent the damage of the mould, there is a
193 stage named anomaly detection (AD) to assure that there is no metal chip on the die before the contact
194 of the die and the punch. Seen from the slider displacement of AD stage in Fig.1, the movement speed
195 of the slider should be decreased smoothly from a high speed to a low speed. In addition, this stage is
196 also a transition phase between the FA stage and the FB stage because the huge difference of the
197 movement speed between the FA stage and the FB stage. In all, the function of this stage is to keep the
198 processing safety and be a transition phase for smoothly fineblanking the sheet metal. Hence, the

199 hydraulic system of the stage should possess the excellent speed regulation ability.

200 The fineblanking stage (FB) is the most important stage which finally achieves the workpiece. To
201 ensure the high quality of the workpiece, the cutting speed should meet the minimum the clean cutting
202 surface about 15~20 mm/s. Hence, the movement speed of the slider should be further decreased while
203 entering into this stage. During this stage, the die and punch with small gap cut the sheet metal and
204 huge force load acts on the main cylinder. In the FB stage, the hydraulic system should provide enough
205 cutting force to overcome the resistance force of cutting the materials steadily. In general, the cutting
206 force can reach hundreds tons and changed with the slider displacement because of the materials
207 characteristic. According to the previous research, the cutting force increases sharply at the beginning
208 of the contact between the die and the punch. Later, it increases nearly linear with the slider
209 displacement in a very short time because of the elastic deformation stage of the material. Then, it
210 keeps at a high level and decreases slowly once the fineblanking stroke is over half. At the end of the
211 FB stage, the cutting force decreases sharply until zero. During this stage, the hydraulic system suffers
212 from huge external disturbance which is a big challenge. In addition, it also needs to provide huge
213 energy for overcoming the deforming energy of the material. In all, the hydraulic system should
214 possess good robustness and disturbance rejection ability to keep steady cutting speed and large power
215 supply.

216 After the FB stage, the high pressure oil is stored in the hydraulic working cylinder. If the high
217 pressure oil is drained into the tank directly, the huge hydraulic vibration will be generated due to the
218 huge pressure difference between the input and the output of the valve. In addition, the hydraulic valve
219 of the hydraulic cylinder is not easy to open because of the high pressure in the cylinder. To avoid this,
220 there should be a transition to release the high pressure steadily that is the pressure unloading stage

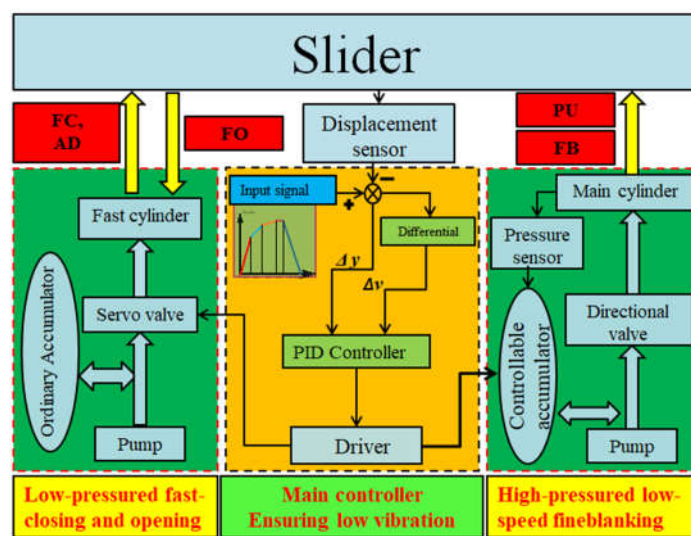
221 (UP). Hence, The UP stage is designed to release the high pressure of the hydraulic cylinder after the
 222 FB stage, which requires the hydraulic system to possess the independent unloading pressure circuit.

223 The fast opening stage (FO) is used to open the mould. Similar with the FC stage, the movement
 224 speed of the slider should be high to reduce the time interval, which is important to improve the
 225 production efficiency. Hence, this stage requires the hydraulic system to be equipped with large flow
 226 supply and excellent dynamic response.

227 In all, from the perspective of fineblanking processing, the requirements of the hydraulic system
 228 can be concluded as follows: the hydraulic system should be designed with the functions of fast
 229 response, huge oil flow supply, high robustness, independent unloading pressure function at the same
 230 time.

231 *2.2 System configuration*

232 To meet the demanding requirements of hydraulic accumulator and achieve the energy saving, this
 233 study proposed a double-stages pressure hydraulic system with a novel controllable accumulator shown
 234 as Fig. 2.



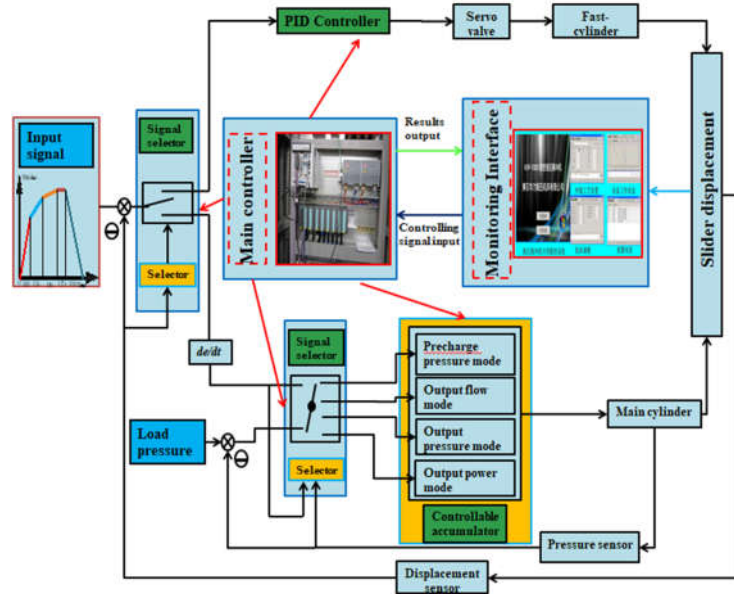
235
 236 Fig. 2. Simplified diagram of main hydraulic system.

237 As shown in Fig. 2, the whole hydraulic system comprises four parts:1) Movements part-the

238 slider. 2) Low-pressured power supply for the fast-closing and opening of the mould. 3) Main
239 controller for ensuring low vibration. 4) High-pressured power supply with controllable accumulator
240 and pressure unloading circuit for low-speed fineblanking steadily. Because the load of the FC, AD, FO
241 stages is only the gravity of the slide, smaller than the blanking force, the low-pressured power supply
242 circuit is suitable for the fast cylinder system. Due to the smaller diameter of the fast cylinder, the
243 low-pressured power supply circuit with small oil flow supply is able to achieve fast-opening and
244 closing mould during the FC, AD, FO stages, which is significant to achieve the balance of the supply
245 and demanded energy. In addition, this low-pressured power supply circuit adopts fixed displacement
246 pump and the servo valve to achieve fast dynamic response. Considering huge overflow dissipation, an
247 ordinary hydraulic accumulator is installed to adjust the energy relationship of this three stages.

248 Because of the fineblanking force can reach hundreds tons, the diameter of the main cylinder
249 should be big enough to overcome the fine blanking force. However, considering the installation space
250 of the fineblanking press and materials saving, the pressure level of this circle should be high to reduce
251 the diameter of the main cylinder. Because the fineblanking force is not constant, the traditional
252 valve-controlled system with fast dynamic response cannot change the supply pressure, which has
253 caused great energy waste. To solve this problem of great energy waste and maintain fast dynamic
254 response, this study proposed a novel controllable accumulator applied on the high-pressured circuit to
255 improve the working performance and improve the energy efficiency by involving four working
256 modes.

257 In addition, the high-low pressured hydraulic system should be worked under the control of the
258 double-loops controller as shown Fig. 3.



259

260

Fig. 3. Schematic of the low-high pressured system controller.

261

Seen from Fig. 3, the whole controller is divided into two parts: fast cylinder circuit controller

262

and main cylinder circuit controller. The former is designed for the low-pressured system and works in

263

the FC, AD, FO stages. The feedback signal is the slider displacement, which is compared with

264

designed slider displacement. After that, the displacement error and velocity error are input to the PID

265

controller for controlling the servo valve. The high robustness of this control algorithm can ensure the

266

high working performance of the fast approaching cylinder system. The latter is designed for the

267

high-pressured system and works during the FB and UP stage. Different with the former controller,

268

there is another feedback that is the bottom pressure of the main cylinder. Through the comprehensive

269

signal selector, the working mode of the controllable accumulator is determined to match the

270

demanding requirements of the FB stage.

271

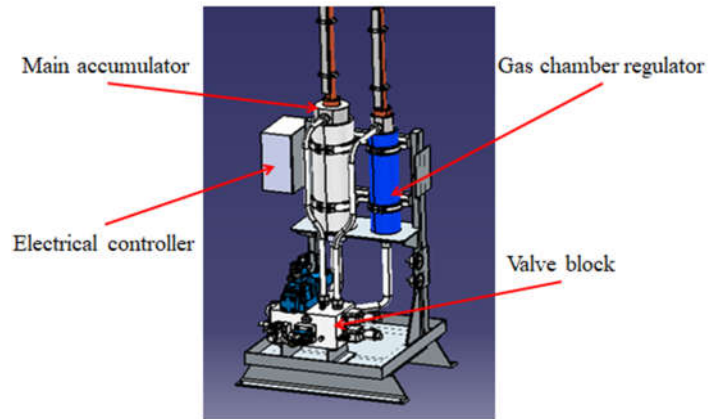
2.3 Controllable accumulator introduction

272

As seen from Fig. 4 and Fig. 5, this novel controllable accumulator mainly comprises four parts:

273

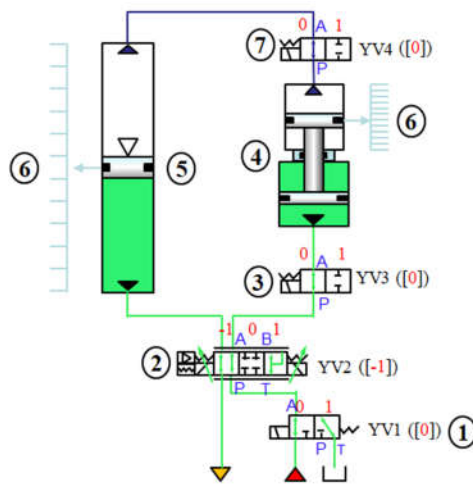
- 1) Main accumulator. 2) Gas chamber regulator. 3) Valve block. 4) Electrical controller.



274

275

Fig. 4. Virtual assembly structure of controllable accumulator.



276

277 1- Two-position hydraulic valve (YV1), 2 - Three-position proportional valve (YV2), 3- High-speed

278 on-off hydraulic valve (YV3), 4- Gas chamber regulator, 5- Main piston hydraulic accumulator, 6-

279 Displacement sensors, 7- High-speed on-off pneumatic valve (YV4)

280

Fig. 5. Hydraulic schematic of the controllable accumulator .

281 In the controllable accumulator, the gas regulator is used to adjust the gas pressure of the main

282 accumulator. Through combining the controlling of these four valves, this novel accumulator can

283 achieve four working modes: 1) Output pressure controlling mode; 2) Precharge pressure controlling

284 mode; 3) Output flow controlling mode; 4) Output power controlling mode.

285 1) Output pressure controlling mode: the target of this mode is to control the output pressure to

286 match the load pressure, which is similar with load sensing system for saving energy.

287 2) Precharge pressure controlling mode: this mode often works in the charging process of the
288 controllable accumulator. By adjusting the piston position of the gas volume regulator, the prescharge
289 pressure of the main accumulator can be changed, which directly influences the capacity of energy
290 storage and the main function.

291 3) Output flow controlling mode: this mode works in the discharging process, which can achieve
292 the designed oil flow output by through controlling three-position proportional valve. This is
293 significant to achieve the precisely controlling of the velocity of the actuator.

294 4) Output power controlling mode: In this mode, the controllable accumulator can achieve the
295 designed power output to match the demand power of the load.

296 The usage core of the controllable accumulator is to reasonably select the working mode
297 according to the requirement of the load characteristics and the working performance. Hence, a detailed
298 select strategy considering the actual working condition is made to achieve high working performance
299 and high energy efficiency as shown Fig. 6.

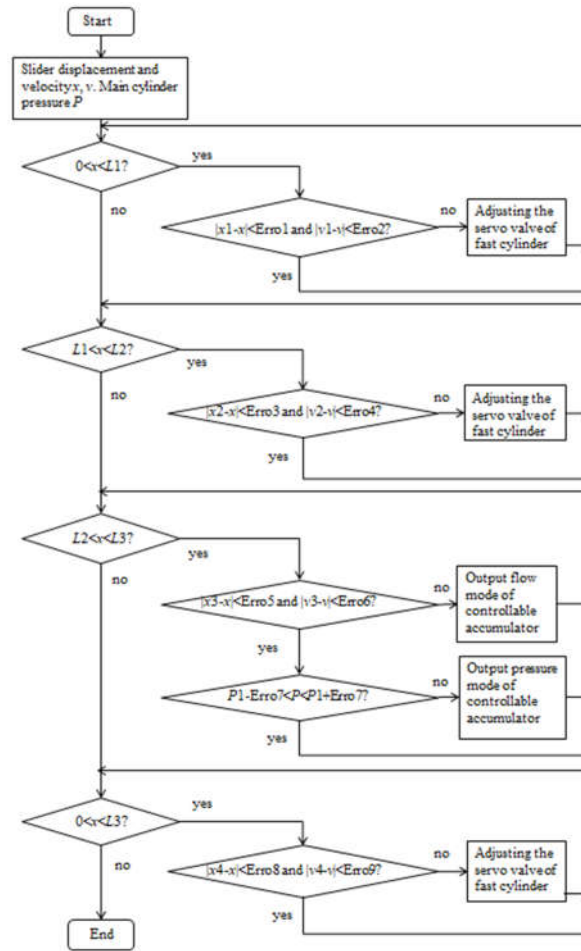


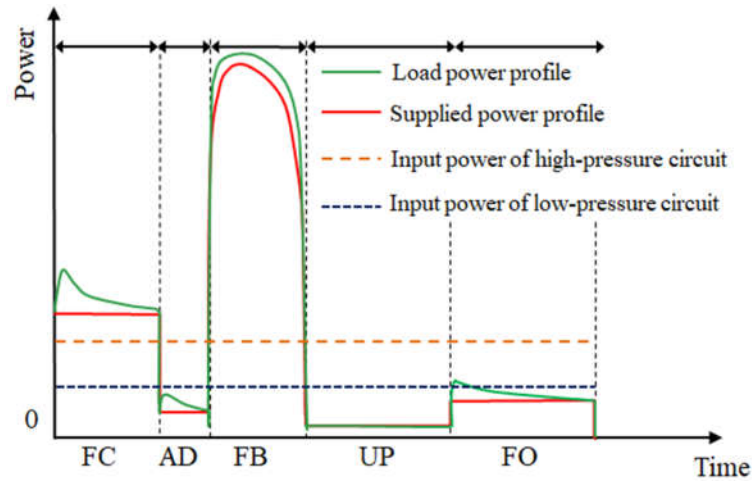
Fig. 6. Principle of selector in the main controller

Seen from Fig. 6, during the FC, AD, FO stages, the designed displacement and velocity of the slider are achieved by controlling the servo valve of the fast cylinder system. Through the feedback signal, the close loop controller can ensure the high accuracy of the designed target with tolerant error. In the FB stage, the designed displacement and the velocity of the slider should be ensured to meet the primary requirements of fineblanking the materials by changing into the output flow mode of the controllable accumulator. Once it meets, the controllable accumulator will start the output pressure mode to match the load pressure for saving energy.

2.4 Energy characteristic of proposed system

As shown in Fig. 2, the main parts of the proposed system are the low-pressured circuit and the high-pressured circuit. During this two circuits, they have the independent power supply units and

312 energy regulators. For the low- press circuit, the power supply unit is the ordinary motor with fixed
313 displacement pump, which belongs to constant output flow system. During the FC, AD, UP, FO Stages,
314 the system load mainly comes from the gravity of the slider. In addition, the movement speed of each
315 stage is constant. Hence, the load power of each stage is also constant. Generally, there are two
316 different methods to match this type of load power demand. The first one is to keep the appropriate
317 constant supply pressure for meeting the load pressure of different stages for reducing overflow of
318 energy consumption. However, this kind of method loses the advantages of the fast response speed,
319 which is unaccepted for the hydraulic fine blanking press. The second method is to adapt the
320 accumulator to regulate the power relationships between these stages, which is also able to increase the
321 system response speed. The input power of the low pressures circuit is lower than the load power of the
322 FA stages and higher than the load power of the AD, UP, FO stages. The function of the ordinary
323 accumulator is to absorb the extra energy of the AD, UP, FO stages and release the storage energy
324 during the FC stages, which is helpful to reduce the installed power of the motor in the low pressure
325 circuit. However because of the output pressure decreasing with the output oil of the ordinary
326 accumulator, at the beginning of draining stage, a peak supply power comes up and the output power of
327 the ordinary accumulator will decrease with the oil flow output constantly, Seen from the supplied
328 power profile in Fig. 7. As for the FB stage, the load power is super-high and changeable, which will
329 lead to great energy waste if adopting the ordinary accumulator. The controllable accumulator has four
330 working modes, which can adjust its output pressure to track the load power profile automatically.
331 Similar with the ordinary accumulator in the low pressure circuit, this controllable accumulator only
332 works in the FB stages and absorbs the extra energy during other stages. In all, the supplied power
333 should higher than the load power for ensuring the normal working of the fineblanking processing.



334

335

Fig. 7. The relationships between the supplied power and the load power.

336

3. Energy mathematical model

337

For the hydraulic system, the input energy is mainly the electricity from three-phase electrical

338

source, which is initially converted into the static pressure energy and kinetic energy of oil fluid by the

339

hydraulic pump and finally transformed into the kinetic energy of the slider to forming the workpiece.

340

In addition, a very small part comes from the extra source such as the atmospheric pressure and the

341

gravity. Cooperating with the appropriate controlling strategy, the transfer direction and the amplitude

342

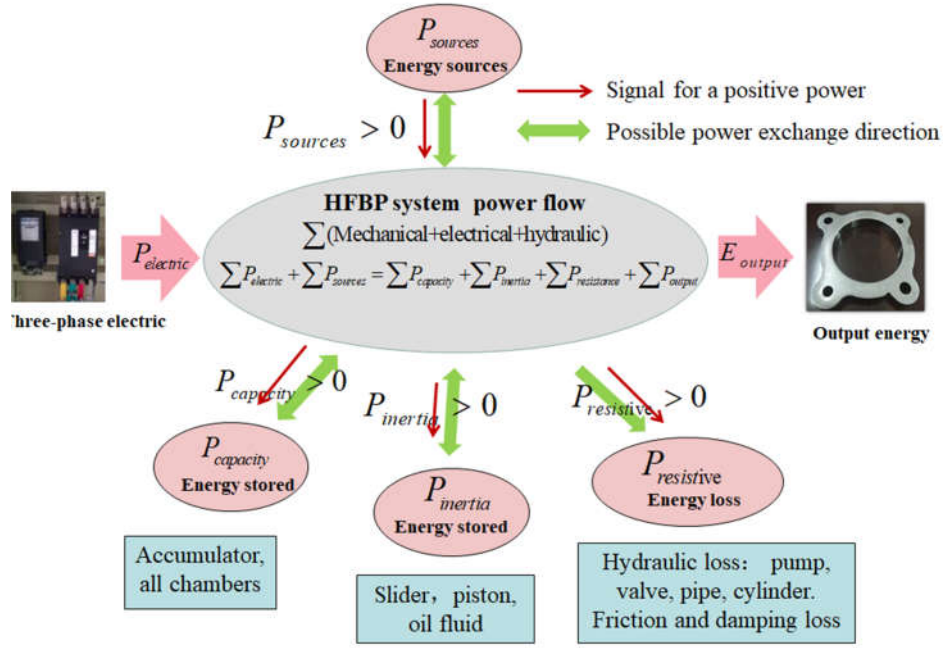
of the energy flow can be precisely controlled to achieve high working performance through these

343

valves. In the energy transmission system, the energy forms of consumption end comprise four parts:

344

capacity energy, inertia energy, resistance energy, and output energy, which can be expressed by Fig. 8.



345

346

Fig. 8. Energy flow chart of hydraulic system.

347

In hydraulic system, there are amounts of oil chambers such as hydraulic accumulators, the

348

cylinder oil chambers, pipes chamber and the valve chambers, which can store the high-pressured oil.

349

In actual, the interaction relationship between these chambers and the main system is mutual. All these

350

storage energy will be released and returned to the main system. However, some capacity energy are

351

utilized for forming workpiece such as the hydraulic accumulator and some are wasted in the form of

352

thermal energy such as the high-pressured energy of the cylinder chamber. For the general oil chamber,

353

the capacitive power of the fluid volume can be computed as follows:

354

$$P_{capacity} = p_{chamber} \cdot q_{inflow} \quad (1)$$

355

$P_{capacity}$ is the capacitive power of fluid volume. $p_{chamber}$ is the chamber pressure. q_{inflow} is the

356

inflow oil into the chamber.

357

Similar to the electric capacitor, these chambers can function as energy storage and vibration

358

reduction, which is important to the working performance of the hydraulic system as well to the system

359

energy consumption characteristic.

360 Inertial energy is due to the motion of the body. For the hydraulic system, the most important
 361 part is the oil fluid. The oil fluid contains two typed energy, which are the static pressure and kinetic
 362 energy, respectively. For the machine, the proportion of these two type energy determines the working
 363 mode of the power transmission system. For the hydraulic pressure system, the capacitive energy
 364 accounts for the major. Relatively, the energy of hydrostatic system is transmitted by the inertial energy
 365 of oil fluid. For the hydraulic system, the oil flows in the pips or the holes. Hence, the inertial of the
 366 moving oil fluid can be calculated by Eq. (2):

$$367 \quad P_{iner-oil} = \frac{L}{S \cdot (1 + p_{mean} \cdot r_{comp})^2} \cdot \rho_{oil} \cdot Q_v \cdot \frac{dQ_v}{dt} \quad (2)$$

368 L is the length of the pipe or hose. S is the cross section arear of the pipe or hose. R_{comp} is the
 369 radial wall compliance of the pipe or hose. p_{mean} is the mean pressure of the pipe or hose. ρ_{oil} is density
 370 at the mean pressure. Q_v is the volumetric flow rate at the mean pressure.

371 In addition, for mechanical system, the piston moves with huge inertial energy, which can be
 372 expressed by Eq. (3).

$$373 \quad P_{iner-mech} = m \cdot a \cdot v \quad (3)$$

374 m is the body mass. a is the body acceleration. v is the body velocity.

375 In hydraulic system, the hydraulic components, such as the motor, the pump, the hydraulic
 376 cylinder, the pipe, the hydraulic valve and the accumulator, are the basic elements of the hydraulic
 377 system as well as the basic units of energy transmission and transformation. When high pressure oil
 378 passes these hydraulic components, energy dissipation will be generated because of resistance effect.
 379 Additionally, it should be pointed out that the

380 In Author Xu et al., (2019) , the motor loss p_e , pump volume-mechanical loss $p_{pump-loss}$, pipe local –
 381 rout loss $p_{pipe-loss}$, valve throttling loss $p_{valve-loss}$, cylinder leakage loss $p_{cylin-loss}$, and overflow loss $p_{overf-loss}$

382 are expressed as follows.

$$383 \quad p_e = p_n \left(k_1 + \frac{k_2 p_u}{p_n} \right) \quad (4)$$

$$384 \quad p_{pump-loss} = p_u (1 - \eta_v \eta_m) = p_u \left[1 - \left(1 - \frac{1000 C_s \Delta q}{\mu n_p} \right) \left(\frac{T_{out}}{T_{out} + T_{fic}} \right) \right] \quad (5)$$

$$385 \quad p_{pipe-loss} = p_j + p_f = \lambda \frac{d}{l} \frac{\rho v_t^2}{2} Q_t + \xi \frac{\rho v_t^2}{2} Q_t \quad (6)$$

$$386 \quad p_{valve-loss} = c\pi \left(d_c - \frac{1}{2} x_0 \sin 2\alpha \right) \sin \alpha \sqrt{\frac{2(P_a - P_b)}{\rho}} (P_a - P_b) \quad (7)$$

$$387 \quad p_{cylin-loss} = C_{ic} (p_1 - p_2)^2 + B_c A_j \frac{dy}{dt} \quad (8)$$

$$388 \quad p_{overf-loss} = p_s q_d \quad (9)$$

389 Hence, the total power loss $P_{loss-hydra}$ of hydraulic system can be expressed by Eq. (10)

$$390 \quad P_{loss-hydra} = p_e + p_{pump-loss} + p_{pipe-loss} + p_{valve-loss} + p_{cylin-loss} + p_{overf-loss} \quad (10)$$

391 For the body motion such as the piston and the slider, because of the friction and damping, some
392 energy will be dissipated and can be calculated by Eq. (11):

$$393 \quad P_{loss-mech} = F_{friction} \cdot v = C_{damp} \cdot v^2 \quad (11)$$

394 Hence, the total resistive power is :

$$395 \quad P_{resistive} = P_{loss-hydra} + P_{loss-mech} \quad (12)$$

396 Based on the energy conservation law of an energy system, we can get Eq. (13):

$$397 \quad \sum P_{electric} + \sum P_{sources} = \sum P_{capacity} + \sum P_{inertia} + \sum P_{resistive} + \sum P_{output} \quad (13)$$

398 For the HFBP, the sources energy refers to the atmosphere pressure and the gravity. The
399 previous covers to all the components and the united force is zero at the same time. So it can be
400 ignored. The direction of the latter is down, which affects the relationship between the supplied
401 and the demanded power although the total input energy from the gravity source at one cycle is
402 zero considering the regular motion of piston and the slider of the machine. Hence, the Eq. (13)
403 can be simplified as Eq. (14):

404
$$\sum P_{electric} + \sum P_{gravity} = \sum P_{capacity} + \sum P_{inertia} + \sum P_{resistive} + \sum P_{output} \quad (14)$$

405

406 **4. Parameters design of two accumulator**

407 In the proposed system, the most important part is to design the parameters of two
 408 accumulators especially the controllable accumulator. Based on the requirements of the working
 409 performance and the minimum energy consumption principle, the main parameters of this two
 410 accumulators are calculated.

411 *4.1 key parameters design of the ordinary accumulator*

412 Actually, the ordinary accumulator cannot generate the extra oil. In the low-pressured
 413 circuit, the total output oil volume from the low-pressured pump should fill the total volume of the
 414 fast cylinder. Hence, the average output flow rate q_{m1} of the low-pressed pump in one cycle can be
 415 calculated by Eq. (15):

416
$$q_{m1} = \frac{V_{fast-rod} + V_{fast-rodless}}{T} = \frac{v_1 A_{fast-rodless} \Delta t_1 + v_2 A_{fast-rodless} \Delta t_2 + v_5 A_{fast-rod} \Delta t_5}{\sum_{i=1}^5 \Delta t_i} \quad (15)$$

417 q_{m1} is the average output flow rate q_{m1} of the low-pressed pump (L/min). $V_{fast-rod}$ and
 418 $V_{fast-rodless}$ are the rod chamber volume and the rodless chamber volume of the fast cylinder (L).
 419 $A_{fast-rod}$ and $A_{fast-rodless}$ are the rod chamber volume and the rodless area of the fast cylinder (mm²). T
 420 is the total time of each working cycle (s). v_i (mm/s) and Δt_i (s) are the movement speed and time
 421 interval of the slider during the FC, AD, FB, UP, FO stages, $i \in [1,5]$.

422 During the FC, AD and FO stages, the oil flow from the low-pressed pump is insufficient
 423 to drive the high speed movement of the slider. Hence, the accumulator should provide the extra
 424 oil flow to the fast cylinder and the effective working volume ΔV_I of this accumulator can be

425 calculated:

$$426 \quad \Delta V_1 = (v_1 A_{fast-rodless} \Delta t_1 + v_2 A_{fast-rodless} \Delta t_2 + v_5 A_{fast-rod} \Delta t_5) - q_{m1} (\Delta t_1 + \Delta t_2 + \Delta t_5) \quad (16)$$

427 During the FB, UP and WT stages, all the input energy of the pump should enter the
428 accumulator ideally, which belongs to the capacity energy. Hence we can get following equation:

$$429 \quad \int_0^{\Delta t_3 + \Delta t_4} \sqrt{3} UI \cos(\alpha_1) dt - \int_0^{\Delta t_3 + \Delta t_4} P_{capacity} dt = 0 \quad (17)$$

430 U (V) and I (A) are the input voltage and current of the electric motor, respectively. α_1 is the
431 power factor of the motor;

432 On combining this with Eqs. (18)–(20):

$$433 \quad \int_0^{\Delta t_3 + \Delta t_4 + \Delta t_6} P_{capacity} dt = \frac{p_{min1} V_{min1}}{n_0 - 1} \left[\left(\frac{p_{max1}}{p_{min1}} \right)^{\frac{n_0 - 1}{n_0}} - 1 \right] \quad (18)$$

$$434 \quad p_{01} V_{01}^{n_0} = p_{min1} V_{min1}^{n_0} = p_{max1} V_{max1}^{n_0} = c_1 \quad (19)$$

$$435 \quad V_{01} = \frac{\Delta V_1}{\left(\frac{p_{01}}{p_{min1}} \right)^{\frac{1}{n_0}} - \left(\frac{p_{01}}{p_{max1}} \right)^{\frac{1}{n_0}}} \quad (20)$$

436 p_0 , p_{min} , and p_{max} are the pre-charge pressure, minimum working pressure, and maximum working
437 pressure (bar) of the ordinary accumulator, respectively; n_0 is the air polytropic exponent value; and V_0
438 is the total volume of the ordinary accumulator (L).

439 In this study, the parameters p_0 , p_{max} , p_{min} , V_0 , and ΔV of the ordinary accumulator were
440 obtained as 90 bar, 170 bar, 190 bar, 16 L, and 0.5446 L, respectively in the 1000 ton fineblanking
441 press.

442 4.2 key parameters design of the controllable accumulator

443 The controllable accumulator only works in the FB stage and will provide huge oil flow to the
444 main cylinder during this stage. So the effective working volume of the controllable accumulator can

445 be calculated:

$$446 \quad \Delta V_2 = v_3 A_{main} \Delta t_3 - q_{m_2} \Delta t_3 \quad (21)$$

447 For reducing the overflow dissipation, the controllable accumulator should be able to absorb the
448 output oil from other stages. Hence, the ΔV_2 should meet the condition:

$$449 \quad \Delta V_2 = \sum \Delta t_i q_{m_i} \quad (i = 1, 2, 4, 5) \quad (22)$$

450 During these stages, the storage energy of this controllable accumulator is calculated by Eq.

451 (24):

$$452 \quad E_a = \int_0^{\Delta t_1 + \Delta t_2 + \Delta t_4 + \Delta t_5 + \Delta t_6} \sqrt{3} U_2 I_2 \cos(\alpha_2) dt \quad (23)$$

453 U_2 (V) and I_2 (A) are the input voltage and current of the electric motor, respectively. α_2 is
454 the power factor of the motor. E_a is the storage energy capacity of the controllable accumulator.

455 For the controllable accumulator, the effective working volume consisting of two parts the main
456 accumulator and the gas regulator, and the total storage energy can be calculated by Eq.(24) and
457 Eq.(25), respectively.

$$458 \quad \Delta V_2 = V_{02} + V_{m2} - V_1' = V_{02} \left(1 + \frac{V_{m2}}{V_{02}}\right) \left[1 - \left(\frac{P_{02}}{P_{max2}}\right)^{\frac{1}{n_0}}\right] \quad (24)$$

$$459 \quad E_a = \int_{V_1'}^{V_{02} + V_{m2}} P_x dV_x = \frac{V_{02} P_{02} \left(1 + \frac{V_{m2}}{V_{02}}\right)}{1 - n_0} \left[1 - \left(\frac{P_{max2}}{P_{02}}\right)^{\frac{n_0 - 1}{n_0}}\right] \quad (25)$$

460 During the FB stage, the supplied energy from the motor and the controllable accumulator and the
461 demanded energy of the load should obey the energy conservation law based on the Eq.(14):

$$462 \quad E_{electric} + E_a + E_{gravity} = E_{inertia} + E_{resistive} + E_{load} \quad (26)$$

463 In the Eq. (27), the important part is to determine the demanded energy of the load. Though the
464 analysis the forming process of the material, the fineblanking force is related to the fineblanking stroke

465 and can be expressed by Eq. (27).

$$466 \quad F(x) = \begin{cases} \frac{45F_{\max}x}{8X} & 0 \leq x \leq \frac{1}{6}X \\ \frac{-9F_{\max}(x - \frac{1}{3}X)^2}{4X^2} + F_{\max} & \frac{1}{6}X < x \leq X \end{cases} \quad (27)$$

467 X is the thickness of the sheet metal. F_{\max} is the maximum fineblanking force. x is the stroke.

468 Hence, E_{load} can be expressed by Eq.(29):

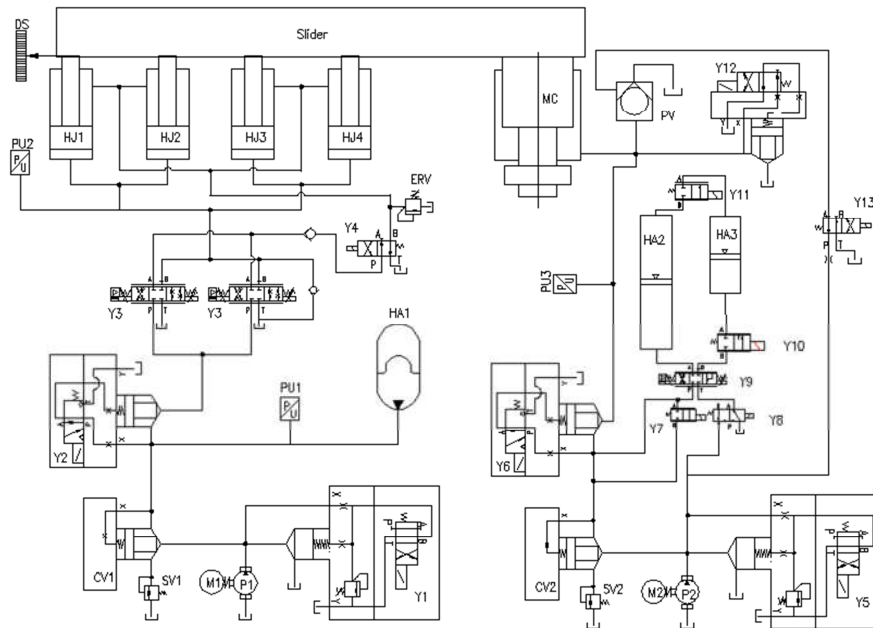
$$469 \quad E_{load} = \int_{\sum_{j=1}^2 \Delta t_i}^{\sum_{j=1}^3 \Delta t_i} F(x(t))v_3(t)dt \quad (28)$$

470 In this study, the parameters p_0 , p_{\max} , p_{\min} , V_0 , and ΔV of the controllable accumulator were
 471 obtained as 100 bar, 230 bar, 190 bar, 16 L, and 12.100 L, respectively in the 1000 ton fineblanking
 472 press. The gas regulator volume is 50.02 L. The maximum storage energy of the controllable
 473 accumulator 760.72 kJ.

474

475 5. Case study

476 According to the schedumatic of the proposed system, a detailed hydraulic pricinple diagram
 477 of 1000 ton hydraulic fineblanking press was designed as Fig .9. The whole diagram comprises
 478 the fast cylinder circuit and the mian cylinder circuit. To avoid the unbalanced torque, there is four
 479 fast cylinders installed on the symmetrical corner of the squarare slider. This circuit takes the servo
 480 valve to achieve speed adjustment of the fast cylinder piston. The main cylinder is a single acting
 481 cylinder with equipping fast charging function and pressre releasing function. The main cylinder is
 482 installed on the center position of the slider shown as Fig. 10.

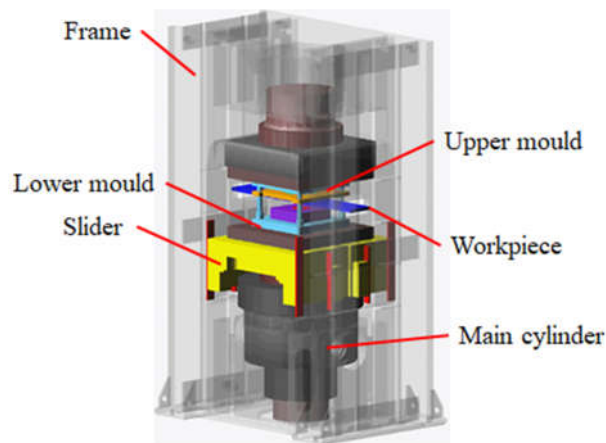


483

484 Y1,Y5- Hydraulic Pressure relief cartridge valve; Y2, Y6- Hydraulic Direction control cartridge
 485 valve; Y3-Hydraulic Servo flow control valve; Y4-Hydraulic Direction control valve; Y7, Y10 -
 486 Hydraulic ON/OFF valve; Y9- Servo flow control valve; Y10-Hydraulic ON/OFF valve; Y11-
 487 Pneumatic ON/OFF valve; Y12- hydraulic pressure unloading valve.

488

Fig. 9. Detailed schedumatic of 1000 ton hydraulic fineblanking press.



489

490

Fig. 10. Assembly virtual structure of 1000 ton hydraulic fineblanking press.

491

According to the principle diagram of 1000 ton hydraulic fineblanking press and the dynamic

492

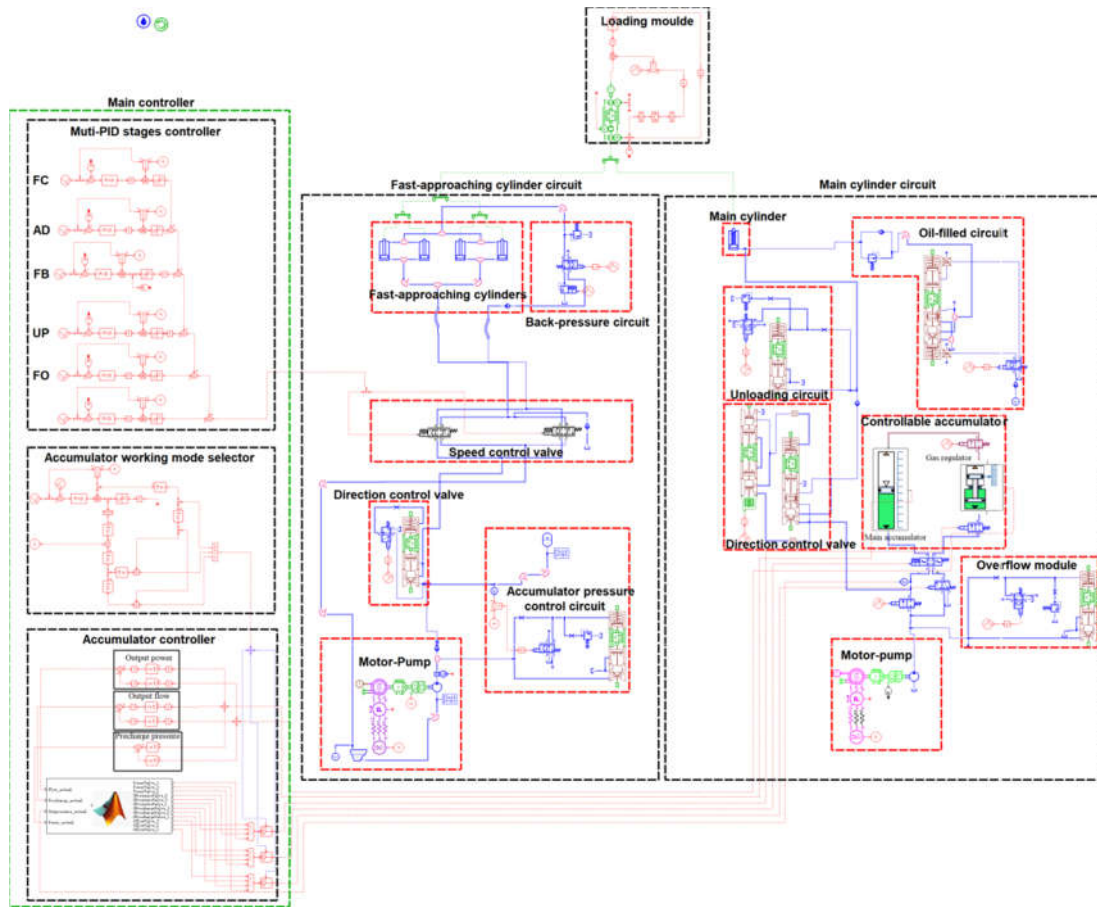
model simulation model with energy consumption analyzing function was built. Combined with

493

Matlab software, some complicated controlling strategies such as the multiple stage PID for the

494 fast cylinder circuit and the Fuzzy PID controller for the controllible accumualtor can be achieved

495 with high precision.



496

497 Fig. 11. Simulation model of 1000 ton hydraulic fineblanking press

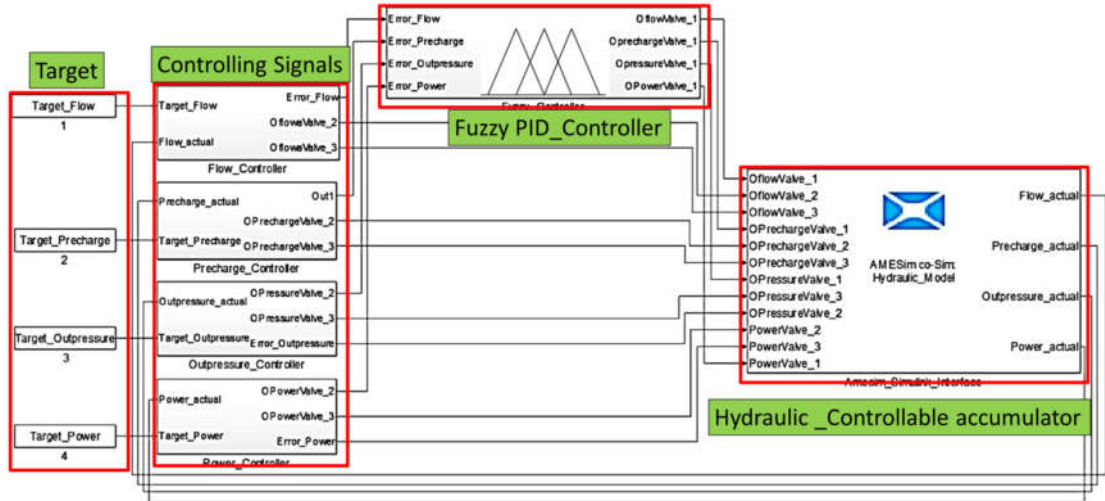
498 Seen from Fig. 11, the whole model comprises the main controller, fast-approaching cylinder

499 circuit module, main cylinder circuit module and the load module. In the load modlue, the

500 experiment fineblaking load was downloaded and acted on the main cylinder circuit in the

501 simulation process. The Fuzzy PID controller for the controllible accumualtor was built on the

502 Matlab-Simulink as shown Fig. 12.



503

504

Fig. 12. Fuzzy PID controller schematic for the controllable accumulator .

505

For the 1000 ton hydraulic press, the main parameters of the simulation model was shown

506

as Table. 1.

507

Table 1. Main parameters in the simulation model.

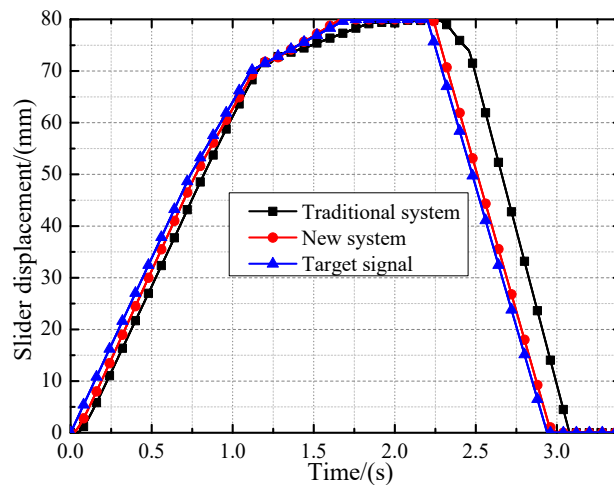
| Circuit | Parameters | Units | Value |
|------------------------|----------------------------|------------------------|-------|
| System parameters | FC stage stroke | <i>mm</i> | 60 |
| | AD stage stroke | <i>mm</i> | 10 |
| | FB stage stroke | <i>mm</i> | 10 |
| | FO stage stroke | <i>mm</i> | 80 |
| | One cycle duration | <i>s</i> | 2.9 |
| | Slide block weight and die | <i>kg</i> | 17500 |
| | Gravity value | <i>m/s²</i> | 9.81 |
| Fast cylinder circuit | Motor speed | <i>r/min</i> | 1440 |
| | Motor power | <i>kw</i> | 40 |
| | Pump displacement | <i>cc/r</i> | 100 |
| | Accumulator volume | <i>L</i> | 16 |
| | Pipe diameter | <i>mm</i> | 32 |
| | Total pipe length | <i>mm</i> | 6800 |
| | Cylinder diameter | <i>mm</i> | 65 |
| Main cylinder circuit | Circuit pressure | <i>MPa</i> | 16 |
| | Motor speed | <i>r/min</i> | 1440 |
| | Motor power | <i>kw</i> | 150 |
| | Pump displacement | <i>cc/r</i> | 250 |
| | Main accumulator volume | <i>L</i> | 100 |
| | Gas regulator volume | <i>L</i> | 50 |
| | Circuit pressure | <i>MPa</i> | 25 |
| Main cylinder diameter | <i>mm</i> | 950 | |

508 **6. Results and discussion**

509 The work load of the fineblanking press is 875 ton, which almost reach the maximum
510 working capacity of this machine. This section analyzes the new system form the aspect of
511 working performance and energy consumption.

512 *6.1 Working performance analysis*

513 The working performance and energy distribution of new system with controllable
514 accumulator was analyzed and some important indices concerning about the system performance
515 was compared with that of the traditional system, seen from Fig. 13 to 17. Actually, for the
516 fineblanking press process, the most important is to ensure the slider to move steadily and follow
517 the target signal accurately. Fig. 13 shows the slider displacement of new system and traditional
518 system.



519

520 Fig. 13. Slider displacement of new system and traditional system.

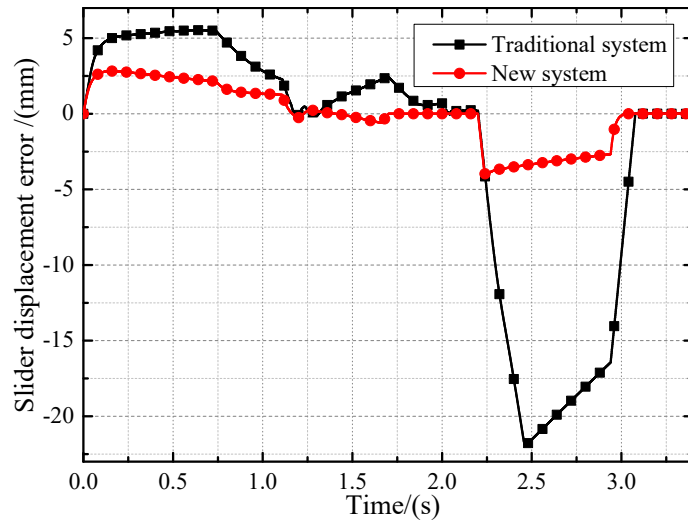
521 Seen from Fig. 13, the time interval of each working cycle is 2.9 s in the new system, which
522 is 0.3s shorter than that of the traditional system. Hence, the production efficiency of the new
523 system is about 10% higher than that of the traditional system. During the FC stage, the slider
524 driven by the fast cylinder gradually gathered speed from 0 mm/s to 70mm/s. However, because of

525 the hysteresis characteristics of hydraulic system, the slider began to move up after 0.1s. Hence,
526 the displacement error between the new system and the target signal has the maximum value about
527 2.5 mm at the beginning of the FC stage and reduced with the time going seen from Fig. 14. When
528 it came into the AD stage, the decent rate of the displacement error increased and the displacement
529 error became comes into near 0 mm at the end of the AD stage seen from the red-line in Fig.14.
530 During the AD stage, the movement velocity of the slider is about 52.5 mm/s, which was well
531 consistent with the target velocity. Compared to the traditional system, the displacement error and
532 the velocity error of the slider of new system were much smaller than that of the traditional system.
533 In addition, the velocity fluctuation range of the slider of the new system was smaller, which is
534 helpful to reduce the pressure fluctuation while the slider came into the FB stage from the AD
535 stage.

536 At the beginning of the FB stages, the movement speed of the slider fluctuated a lot due to
537 the extra load from cutting the workpiece seen from Fig. 15. Because the movement velocity error
538 of the slider reached 30 mm/s which is bigger than the threshold value (20mm/s), the controllable
539 accumulator worked in the output flow mode for ensuring the slider velocity to keep up with
540 target velocity well. During this short time interval, the supplied pressure also fluctuated a lot with
541 the fluctuation of the velocity. The fluctuation duration of the movement speed was last for 0.3 s
542 and then kept at the value of 20 mm/s steadily during the whole FB stage. Correspondingly, the
543 working mode of the controllable accumulator was changed from the output flow mode to the
544 output pressure mode for tracking the load pressure. Seen from the Fig. 17, the supplied pressure
545 of the traditional system is about 230 bar, much higher than the load pressure, which would cause
546 great energy waste. However, in the new system, the supplied pressure can be adjusted to reduce

547 the pressure loss when the controllable accumulator worked in the output pressure mode. Hence,
548 the controllable accumulator can help the hydraulic system to achieve high energy efficiency by
549 controlling the output pressure. During the FB stage, the displacement error of the slider is below
550 0.5 mm, which is very important for ensuring high quality processing for cutting the material.
551 With the help of the controllable accumulator, the displacement and velocity of the actuator could
552 follow the target signal well. This verified that the controllable accumulator could work well on
553 the hydraulic fineblanking press and can greatly improve working performance.

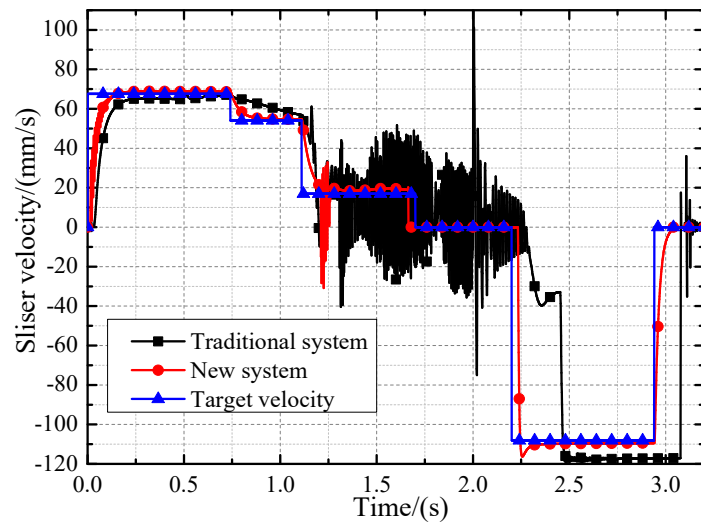
554 The FO stage is designed to release the high pressure main cylinder bottom for the purpose
555 of opening the charge valve installed on the main cylinder. This process would last for 0.5 s
556 until the bottom pressure of the main cylinder reached to 0 bar, which made preparations fast
557 returning of the slider. As shown Fig. 13 and Fig. 15, the slider kept at the top point statically.
558 After this stage, the slider would return the initial point from the top point with high speed about 110
559 mm/s. Similar with the FC stage, there still have the hysteresis problem that the actual movement of
560 the slider was behind the target signal as shown in the Fig. 13 and 15. During the FO stage, the
561 displacement error changed from 4.8mm to 2.5 mm, which was much smaller than that of the
562 traditional system as shown Fig. 14. In addition, the velocity error was kept within a very small range
563 about 0.4mm except for the beginning and the end process of this stage as shown Fig. 16.



564

565

Fig. 14. Slider displacement error of new system and traditional system.

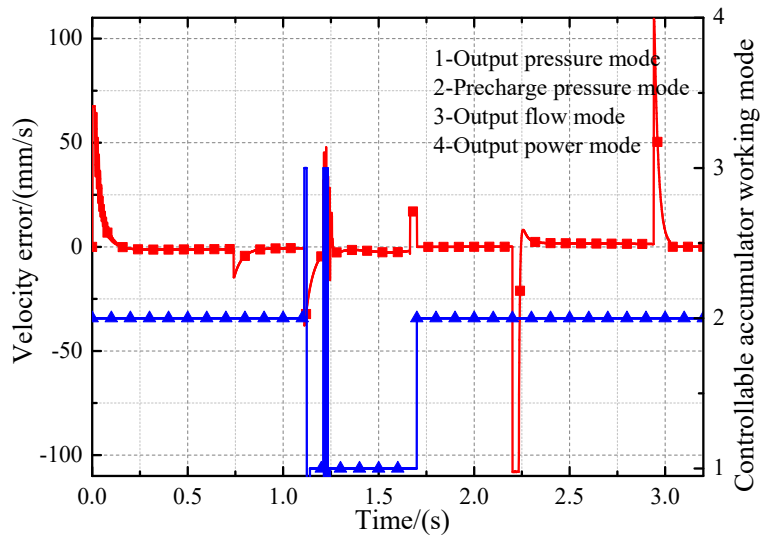


566

567

Fig. 15. Slider velocity of new system, traditional system and target signal.

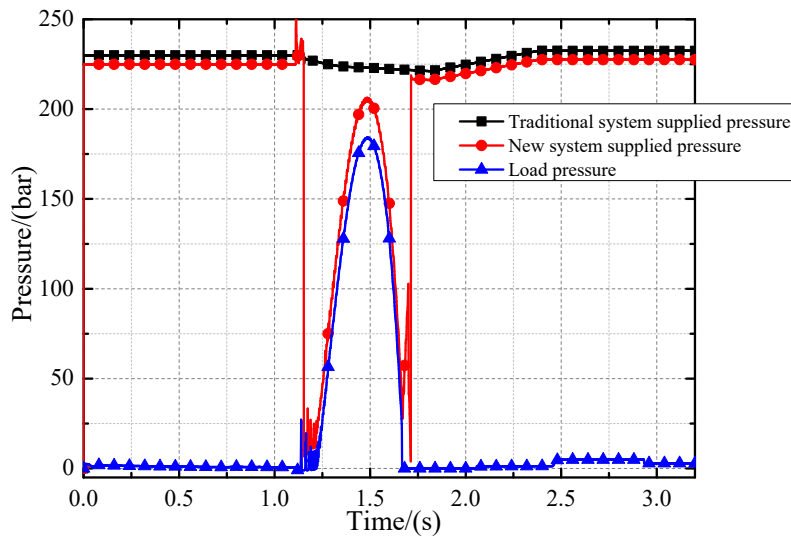
568



569

570 Fig. 16. Relationship between the velocity error and the working mode of controllable

571 accumulator.



572

573 Fig. 17. Load pressure and the supplied pressure of traditional system and the new system.

574 In all, compared to the additional system, the working performance of the new system was

575 improved a lot during each stage, especially in the FB stage. During this stage, the fluctuation

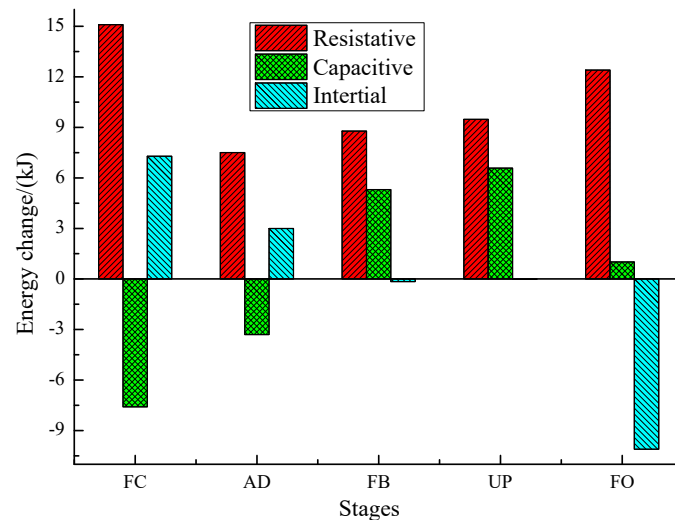
576 range of the displacement error and the velocity error were limited within 0.46 mm and 0.5 mm/s

577 respectively with the help of the controllable accumulator. Additionally, the production efficiency

578 of the new system was also increased by nearly 10% compared to the traditional system.

579 *6.2 Energy dissipation analysis*

580 According to theoretical analysis, the energy type of the whole system can be divided into
 581 three types-resistive energy, capacitive energy and inertial energy. There are two hydraulic circuits
 582 working in the hydraulic fineblanking press, which are the fast cylinder circuit and the main
 583 cylinder circuit, respectively. The former can be taken as the valve-controlled system and three
 584 types of energy were distributed as shown in Fig.18.

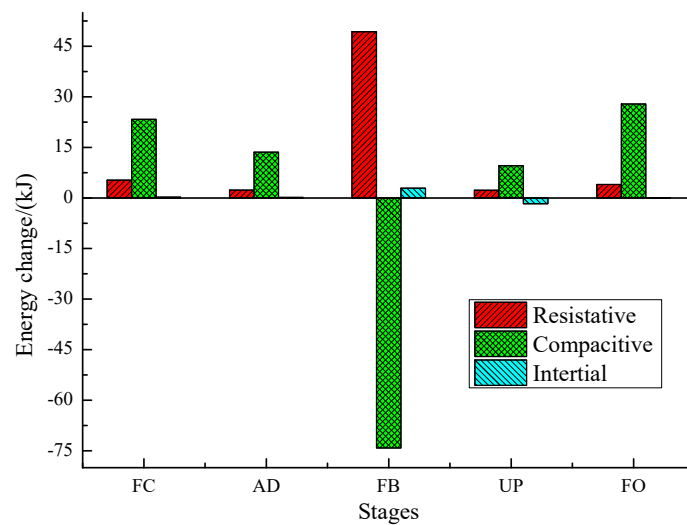


585

586 Fig. 18. Energy change of resistive, capacitive and inertial energy of fast cylinder circuit.

587 Seen from Fig.18, the resistive energy reached 15.1 kJ during the FC stage, which finally was
 588 converted into the thermal energy leading to the increasing temperature of the hydraulic oil.
 589 Actually, most resistive energy was generated from the valve loss, motor loss and pump loss.
 590 During this stage, the ordinary accumulator of the fast cylinder circuit released 7.6 kJ to
 591 supplement the shortage of the pump resource. Hence, the captive energy was negative compared
 592 to the initial status. Because the slider moved up, the gravitational potential energy of the system
 593 was increased with the displacement. In addition, the kinetic energy of the slider was also
 594 increased with the increasing of the velocity. This two parts lead to the inertial energy to be
 595 increased to 7.2 kJ. The next stage, because of the short time duration of the AD stage, these three
 596 types of energy was reduced to half of the FC stage. However, the velocity of the slider with huge

597 mass is decreased from 70 mm/s to 52.5 mm/s, which resulted in a more severe recession of the
 598 inertial energy. When it came into the FB stage, most of energy about 9.1 kJ was consumed in the
 599 form of the motor and pump loss after the ordinary accumulator was charged. Due to the reduction
 600 of the slider velocity, the inertial energy change of the fast cylinder circuit was negative. Similarly,
 601 the energy characteristic of UP stage in the fast cylinder circuit behaved the same trend with that
 602 of the FB stage. During the last stage, the fast cylinder circuit drove the slider to move down with
 603 a high speed, which resulted in the rapid declines of the inertial energy. Because of the valve loss,
 604 the motor loss and pump loss, about 12.3 kJ resistive energy was generated. In all, the resistive
 605 energy accounted for a big part of the total energy of each stage. Hence, it still has a great
 606 potential to save some energy on the premise of ensuring meeting the normal working
 607 requirements in the valve-controlled system.

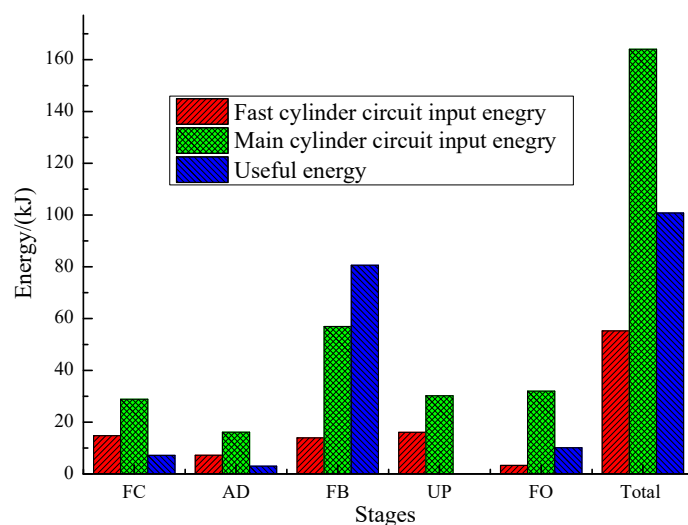


608

609 Fig. 19. Energy change of resistive, capacitive and inertial energy of main cylinder circuit.

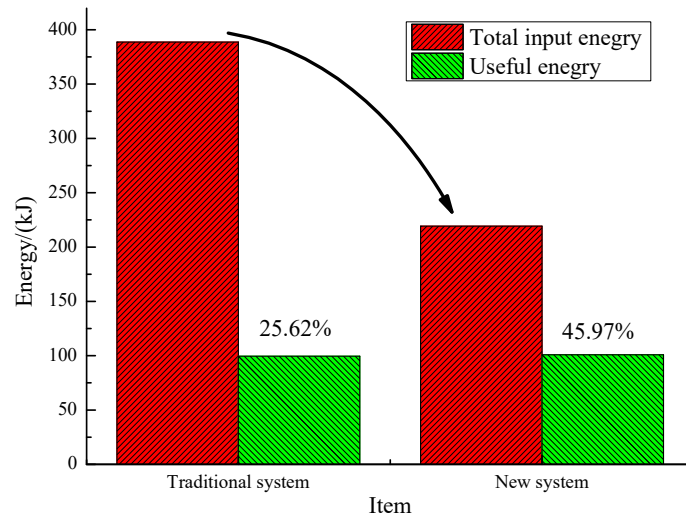
610 The main cylinder circuit only worked in the FB stage. Hence, most energy was converted
 611 and transformed during this stage. Seen from Fig.19, During the FC, AD, UP, FO stages, the
 612 controllable accumulator was charged with little energy consumption as shown in Fig. 19. The
 613 storage energy of the controllable accumulator was released for overcoming the load of

614 fineblanking the workpiece during the FB stage. It can be seen that the controllable accumulate
615 could change the release time and the size of the supplied energy according to the processing
616 requirements. This function of the controllable accumulator caused that the useful energy of the
617 FB stage is higher than the supplied energy from the power resource as shown in Fig. 20. However,
618 during the FB stage, the resistive energy reached 49.32 kJ due to the motor loss, pump loss and the
619 valve loss. Fig. 20 shows the comparison results of this two circuits about the input energy and
620 useful energy of each stage. The total input energy of the main cylinder circuit was about 164.1 kJ,
621 which was almost three times higher than that about 55.26 kJ of the fast cylinder circuit. The total
622 useful energy reached 100.8 kJ, most of which was located in the FB stage. Compared the
623 traditional system, the useful energy of them were almost the same. However, the huge difference
624 of the input between the new system and the traditional system lead to the huge difference of the
625 total energy efficiency as shown in Fig.21. The total input energy of the new system was about
626 219.3 kJ, which saved about 169.4 kJ energy compared the traditional system. Correspondingly,
627 the total energy efficiency of the new system was improved by 20.35% from 25.6% to 45.97%.



628

629 Fig. 20. Energy input and useful energy of each stage in new system.



630

631 Fig. 21. Total input energy and useful energy efficiency of new system and traditional system.

632

633 **7. Conclusion**

634 To improve the work performance and the energy efficiency of the high-end hydraulic press,
 635 a general hydraulic system with double-stage pressure circuit concept was studied from the aspect
 636 of the processing requirements and the energy demand considering make full use of the
 637 controllable accumulator. This new system was applied on the 1000 ton hydraulic fineblanking
 638 press with the working load of 875 ton. Some significant conclusion about this new system can be
 639 drawn as follows.

640 1) Compared to the traditional system, this new system shows better working performance. The
 641 fluctuation range of the displacement error and the velocity error were limited within 0.46 mm and
 642 0.5 mm/s respectively with the help of the controllable accumulator during the fineblanking stage.
 643 This new system solved the huge pressure fluctuation problem while the driving force of the slider
 644 was change with super high load by changing the working mode of the controllable accumulator.
 645 In addition, the production efficiency of the new system is improved by 10% compared to the
 646 traditional system.

647 2. Most energy is input by the main cylinder circuit and consumed in the fineblanking processing.
648 The total energy of the new system is decreased by 169.4 kJ electric energy compared to the
649 traditional system and the total energy efficiency of the new system was improved by 20.35%
650 from 25.6% to 45.97%.

651 In this study, the controllable accumulator is embedded into the hydraulic fineblanking press
652 and improves the working performance and energy efficiency of the machine greatly. Future work
653 will focus on the online energy monitoring of the hydraulic system with adopting some artificial
654 intelligence technology, which is significant to achieve the online energy optimization of the
655 forming machine.

656

657 **Acknowledgements**

658 The authors would like to thanks the Huangshi Huali Metal forming Machine Tool Co., Ltd for
659 providing the technology parameters.

660 **Authors' Contributions**

661 LH was in charge of the whole trial; ZX wrote the manuscript and carried out the simulation; YL
662 assisted with the simulations; XZ was in charge of technical expression and language.

663 All authors read and approved the final manuscript.

664 **Authors' Information**

665 Lin Hua, born in 1962, received his Ph.D. degree in Mechanical Engineering from *Xi'an Jiaotong*
666 *University, China*, in 2000. Dr. Hua is currently a Professor at the *School of Automotive Engineering at*
667 *Wuhan University of Technology, China*. Dr. Hua's research interests include advanced forming and
668 equipment technology.

669 Zhicheng Xu, born in 1993, is currently a Ph.D candidate at *School of Automotive Engineering at*
670 *Wuhan University of Technology, China*. His research interests are green and smart manufacturing.

671 Yanxiong Liu, born in 1985, received Ph.D. degree from Wuhan University of Technology in 2012.
672 From 2010 to 2012, he did the research as a Research Scholar in Purdue University, and currently is an
673 Associated Professor in the School of Automotive Engineering. His research interests lie in the fields of
674 green and smart manufacturing.

675 Xinhao Zhao, born in 1989, is currently a Ph.D candidate at *School of Material science and*
676 *engineering at Wuhan University of Technology, China*. His research interests are green and smart
677 manufacturing.

678

679 **Funding**

680 The authors would like to thank the Fundamental Research Funds for the Central Universities
681 (WUT:501 2019III117CG and 2020-YB-019), 111 Project (B17034), Innovative Research Team
682 Development Program of 502 Ministry of Education of China (No. IRT_17R83) and China Scholarship
683 Council, China (CSC, File, No.201906950038) for the financial supports given to this research.

684 **Competing Interests**

685 The authors declare no competing financial interests.

686 **Author Details**

687 1. Hubei Key Laboratory of Advanced Technology of Automotive Components, Wuhan University of
688 Technology, Wuhan, 430070, China.

689 2. Hubei Collaborative Innovation Center for Automotive Components Technology, Wuhan University
690 of Technology, Wuhan, 430070, China.

691 3. School of Materials Science and Engineering, Wuhan University of Technology, Wuhan, 430070,

692 China

693 4. Department of Mechanical Engineering, University of Wisconsin-Madison, Madison, WI 53706,

694 USA

695

696 **Reference**

697 [1] Gao M, Li L, Wang Q, et al. Energy Efficiency and Dynamic Analysis of a Novel Hydraulic
698 System with Double Actuator[J]. International Journal of Precision Engineering and
699 Manufacturing-Green Technology. 2020, 7(3): 643-655.

700 [2] Bhandari B, Lee K, Lee G, et al. Optimization of hybrid renewable energy power systems: A
701 review[J]. International Journal of Precision Engineering and Manufacturing-Green Technology. 2015,
702 2(1): 99-112.

703 [3] Mianehrow H, Abbasian A. Energy monitoring of plastic injection molding process running with
704 hydraulic injection molding machines[J]. Journal of Cleaner Production. 2017, 148: 804-810.

705 [4] Zhou L, Li J, Li F, et al. Energy consumption model and energy efficiency of machine tools: a
706 comprehensive literature review[J]. Journal of Cleaner Production. 2016, 112: 3721-3734.

707 [5] Yan X, Chen B, Zhang D, et al. An energy-saving method to reduce the installed power of
708 hydraulic press machines[J]. Journal of Cleaner Production. 2019, 233: 538-545.

709 [6] Hua L, Liu Y, Zhuang W, et al. Fineblanking technology and equipment[M]. Wuhan university of
710 technology press, 2015: 332-333.

711 [7] Xu Z, Liu Y, Hua L, et al. Energy analysis and optimization of main hydraulic system in
712 10,000 kN fine blanking press with simulation and experimental methods[J]. Energy Conversion and

713 Management. 2019, 181: 143-158.

714 [8] Lohse H, Weber J. Simulation-Based Investigation of the Energy Efficiency of Hydraulic Deep
715 Drawing Presses[J]. HIDRAVLICNA STISKALNICA(German). 2013, 2(19): 117-124.

716 [9] Xu Z, Liu Y, Hua L, et al. Energy analysis and optimization of main hydraulic system in
717 10,000 kN fine blanking press with simulation and experimental methods[J]. Energy Conversion and
718 Management. 2019, 181: 143-158.

719 [10] Zhao K, Liu Z, Yu S, et al. Analytical energy dissipation in large and medium-sized hydraulic
720 press[J]. Journal of Cleaner Production. 2015, 103: 908-915.

721 [11] Ho T H, Ahn K K. Design and control of a closed-loop hydraulic energy-regenerative system[J].
722 Automation in Construction. 2012, 22: 444-458.

723 [12] H T, K A. Comparison and assessment of a hydraulic energy saving system for hydrostatic drives.
724 Proceedings of the Institution of Mechanical Engineers[J]. Part I: Journal of Systems and Control
725 Engineering. 2011, 1(225): 2134.

726 [13] Yao J, Li B, Kong X. Energy Saving and Control of Hydraulic Press Fast Forging System Based
727 on the Two-stage Pressure Source[J]. Journal of mechanical engineering. 2016, 52(10): 199-206.

728 [14] Jing Y, Bin L, Yu S, et al. Study on Hydraulic Press Fast Forging Energy-saving and Control
729 System Based on Variable Frequency Adjustment[J]. China Mechanical Engineering. 2015(6):
730 749-755.

731 [15] Huang H, Zou X, Li L, et al. Energy-Saving Design Method for Hydraulic Press Drive System
732 with Multi Motor-Pumps[J]. International Journal of Precision Engineering and Manufacturing-Green
733 Technology. 2019, 6(2): 223-234.

734 [16] Li L, Huang H, Zhao F, et al. Analysis of a novel energy-efficient system with double-actuator for

735 hydraulic press[J]. *Mechatronics*. 2017, 47: 77-87.

736 [17] Wang H, Wang H, Zhu T. A new hydraulic regulation method on district heating system with
737 distributed variable-speed pumps[J]. *Energy Conversion and Management*. 2017, 147(147): 174-189.

738 [18] Xu Z, Liu Y, Hua L, et al. Energy improvement of fineblanking press by valve-pump combined
739 controlled hydraulic system with multiple accumulators[J]. *Journal of Cleaner Production*. 2020, 257:
740 120505.

741 [19] Zimmerman J D, Pelosi M, Williamson C A, et al. Energy consumption of an LS excavator
742 hydraulic system[J]. *Proceedings of IMECE2007;2007 ASME International Mechanical Engineering
743 Congress and Exposition*. 2007.

744 [20] Andrea B, Federico C, Mirko P, et al. Energy saving solutions for a hydraulic excavator[J]. *Energy
745 Procedia*. 2017, 126.

746 [21] Lovrec D, Kastrevc M, Ulaga S. Electro-hydraulic load sensing with a speed-controlled hydraulic
747 supply system on forming-machines[J]. *The International Journal of Advanced Manufacturing
748 Technology*. 2009, 41(11-12): 1066-1075.

749 [22] Ge L, Quan L, Zhang X, et al. Efficiency improvement and evaluation of electric hydraulic
750 excavator with speed and displacement variable pump[J]. *Energy Conversion and Management*. 2017,
751 150: 62-71.

752 [23] Yu Y, Ahn K K. Energy Regeneration and Reuse of Excavator Swing System with Hydraulic
753 Accumulator[J]. *International Journal of Precision Engineering and Manufacturing-Green Technology*.
754 2020, 7(4): 859-873.

755 [24] Dang T D, Do T C, Ahn K K. Experimental Assessment of the Power Conversion of a Wave
756 Energy Converter Using Hydraulic Power Take-Off Mechanism[J]. *International Journal of Precision*

757 Engineering and Manufacturing-Green Technology. 2020.

758 [25] Dang T D, Phan C B, Ahn K K. Design and Investigation of a Novel Point Absorber on
759 Performance Optimization Mechanism for Wave Energy Converter in Heave Mode[J]. International
760 Journal of Precision Engineering and Manufacturing-Green Technology. 2019, 6(3): 477-488.

761 [26] Yu Y, Ahn K K. Improvement of Energy Regeneration for Hydraulic Excavator Swing System[J].
762 International Journal of Precision Engineering and Manufacturing-Green Technology. 2020, 7(1):
763 53-67.

764 [27] Jun G, Daqing Z, Yong G, et al. Potential energy recovery method based on alternate recovery and
765 utilization of multiple hydraulic cylinders[J]. Automation in Construction. 2020, 112: 103105.

766 [28] Ge L, Dong Z, Quan L, et al. Potential energy regeneration method and its engineering
767 applications in large-scale excavators[J]. Energy Conversion and Management. 2019, 195(195):
768 1309-1318.

769 [29] Chen Q, Lin T, Ren H, et al. Novel potential energy regeneration systems for hybrid hydraulic
770 excavators[J]. Mathematics and Computers in Simulation. 2019, 163: 130-145.

771 [30] Lin T, Wang L, Huang W, et al. Performance analysis of an automatic idle speed control system
772 with a hydraulic accumulator for pure electric construction machinery[J]. Automation in Construction.
773 2017, 84: 184-194.

774 [31] Yang Y, Li G, Zhang Q. A Pressure-Coordinated Control for Vehicle Electro-Hydraulic Braking
775 Systems[J]. Energies. 2018, 11(9): 2336.

776 [32] Mensing F, Li P Y. Sizing and Optimal Operation of a Power Split Hydraulic Hybrid Drive
777 Train[J]. Proceedings of the International Fluid Power Exhibition, Las, NV, USA. 2226. 2011.

778 [33] Wang R, Gu F, Cattley R, et al. Modelling, Testing and Analysis of a Regenerative Hydraulic

779 Shock Absorber System[J]. *Energies*. 2016, 9(5): 386.

780 [34] Chen Q, Yue X, Geng D, et al. Integrated characteristic curves of the constant-pressure hydraulic
781 power take-off in wave energy conversion[J]. *International Journal of Electrical Power & Energy*
782 *Systems*. 2020, 117: 105730.

783 [35] Pourmovahed A, Otis D R. An Experimental Thermal Time- Constant Correlation for Hydraulic
784 Accumulators[J]. *Transactions of the ASME*. 1990, 112(116): 113-120.

785 [36] Zhao W, Ye Q. Analysis of Dynamic Performance for New Double-bladder Accumulator[J].
786 *Chinese Hydraulic and Pneumatic*. 2018(1): 96-103.

787 [37] Van D V, James D. Constant pressure hydraulic energy storage through a variable area piston
788 hydraulic accumulator[J]. *Applied Energy*. 2013(105): 262-270.

789 [38] Latas W, Stojek J. A new type of hydrokinetic accumulator and its simulation in hydraulic lift with
790 energy recovery system[J]. *Energy*. 2018, 153: 836-848.

791 [39] Liu Y, Xu Z, Hua L, et al. Analysis of energy characteristic and working performance of novel
792 controllable hydraulic accumulator with simulation and experimental methods[J]. *Energy Conversion*
793 *and Management*. 2020, 221: 113196.

794

Figures

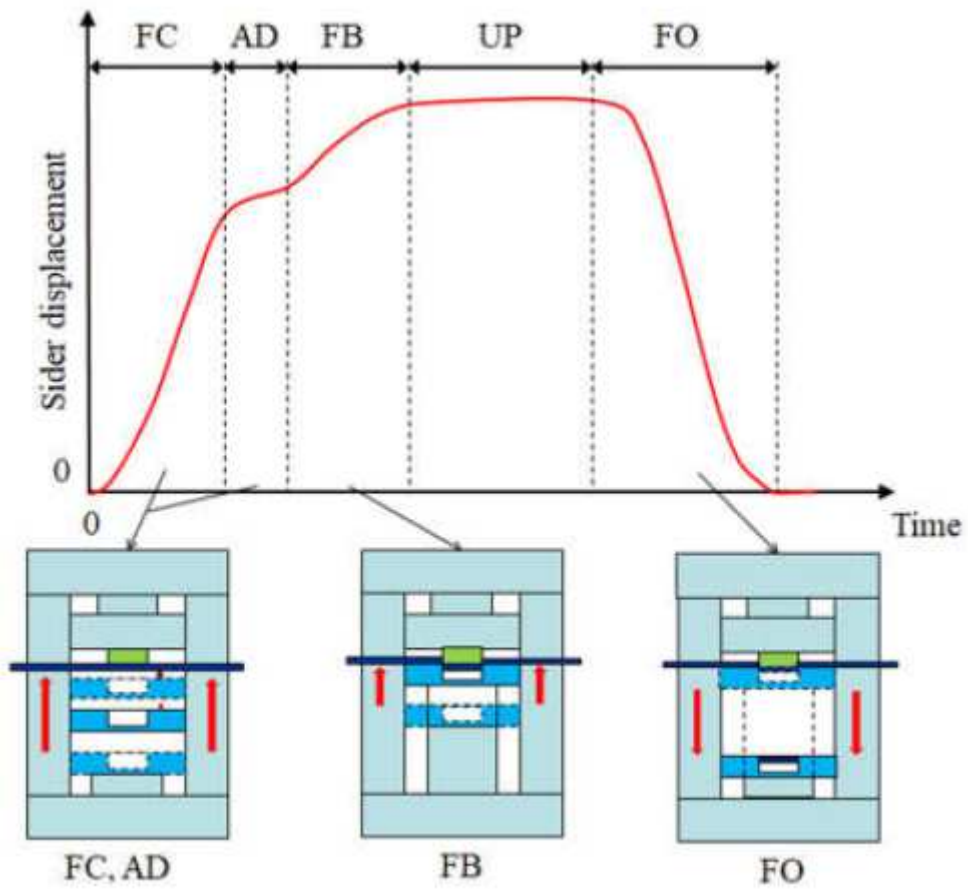


Figure 1

The schedule of work processing and the movement of slider.

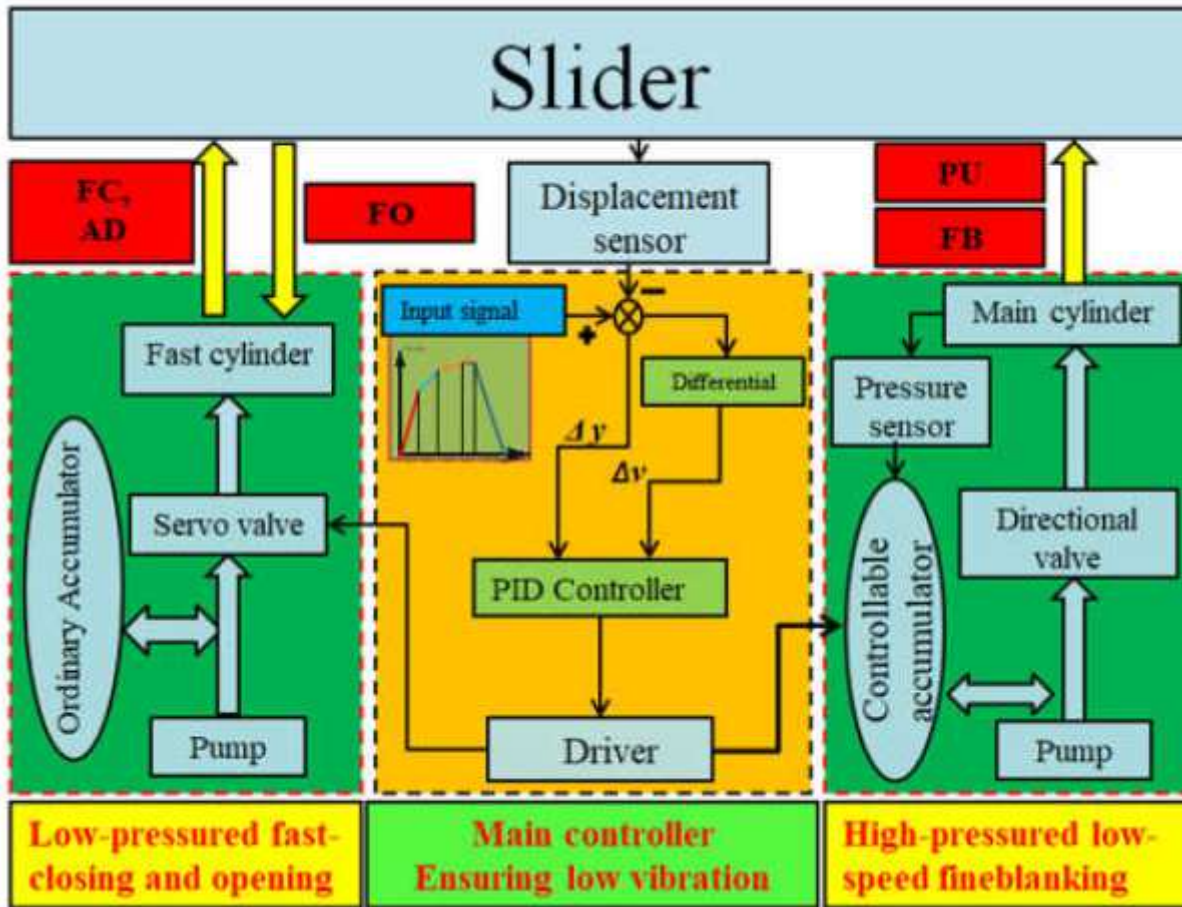


Figure 2

Simplified diagram of main hydraulic system.

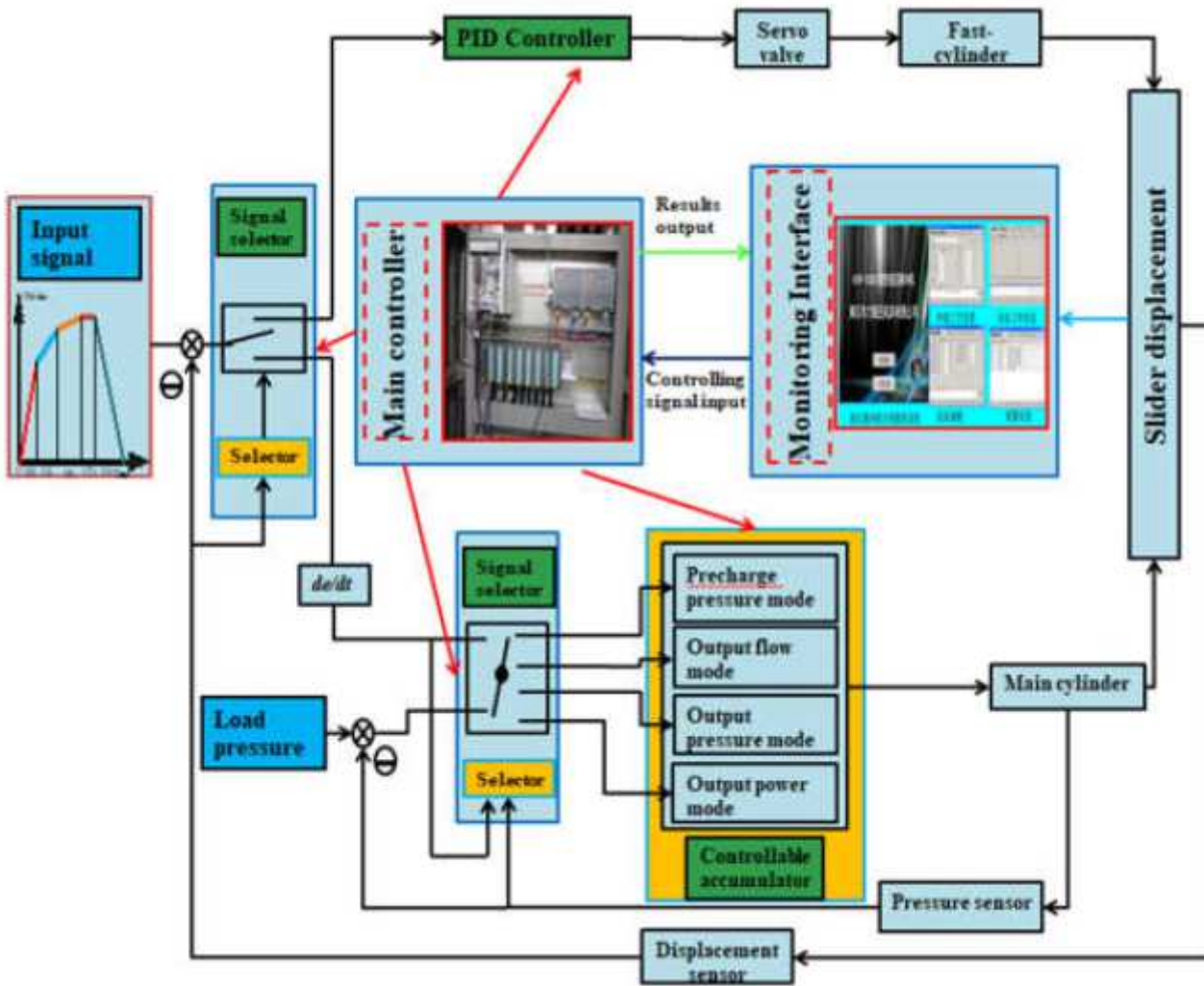


Figure 3

Schematic of the low-high pressured system controller.

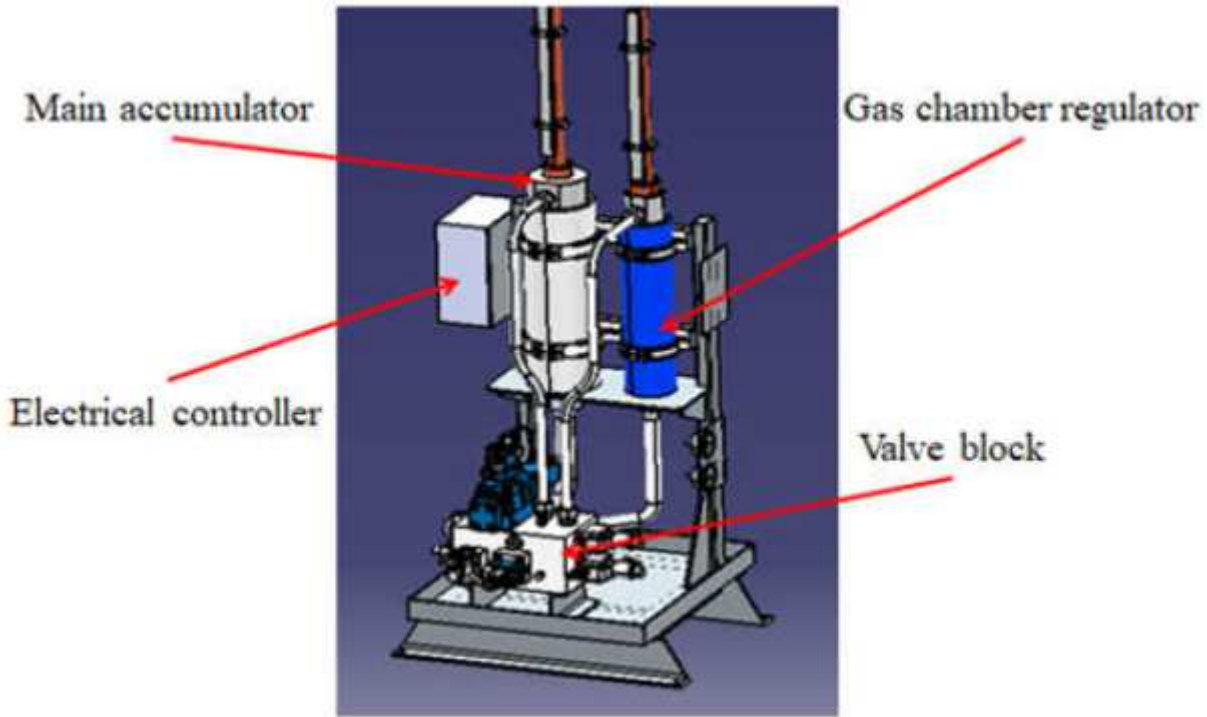


Figure 4

Virtual assembly structure of controllable accumulator.

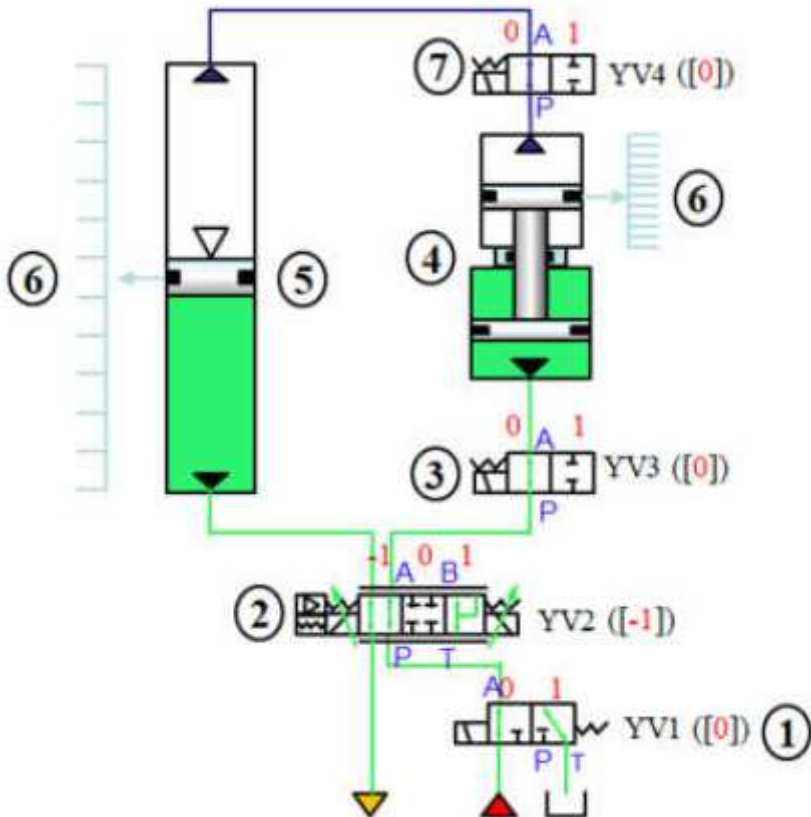


Figure 5

Hydraulic schematic of the controllable accumulator.

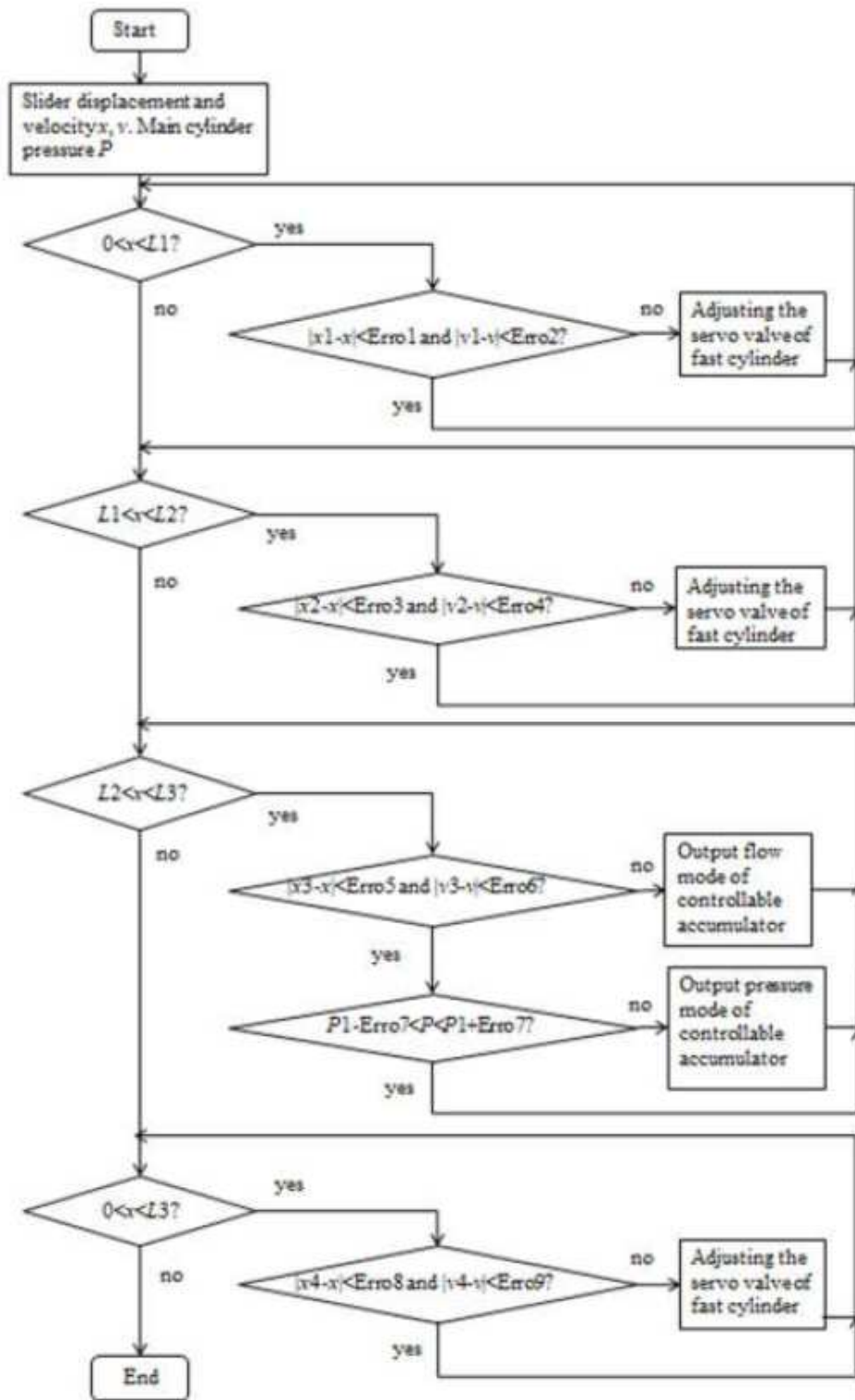


Figure 6

Principle of selector in the main controller

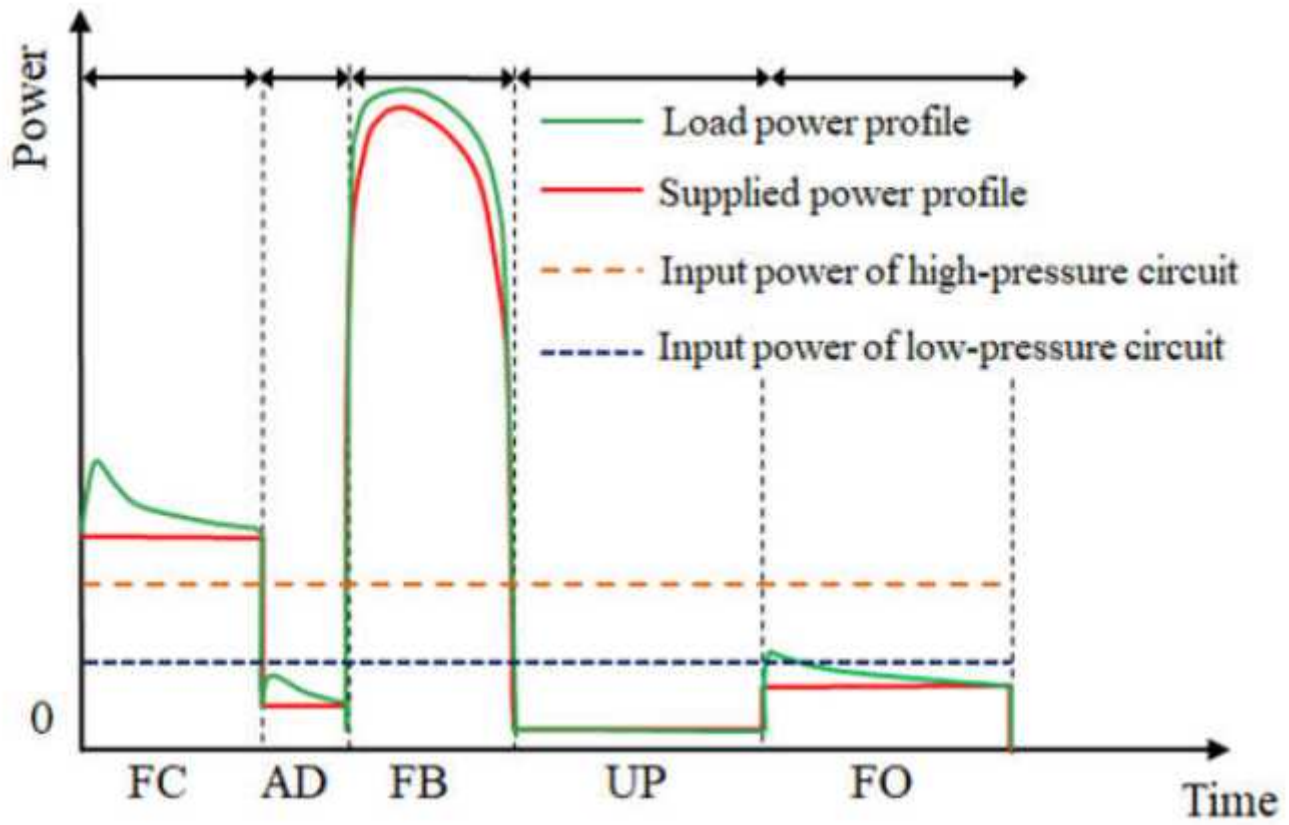


Figure 7

The relationships between the supplied power and the load power.

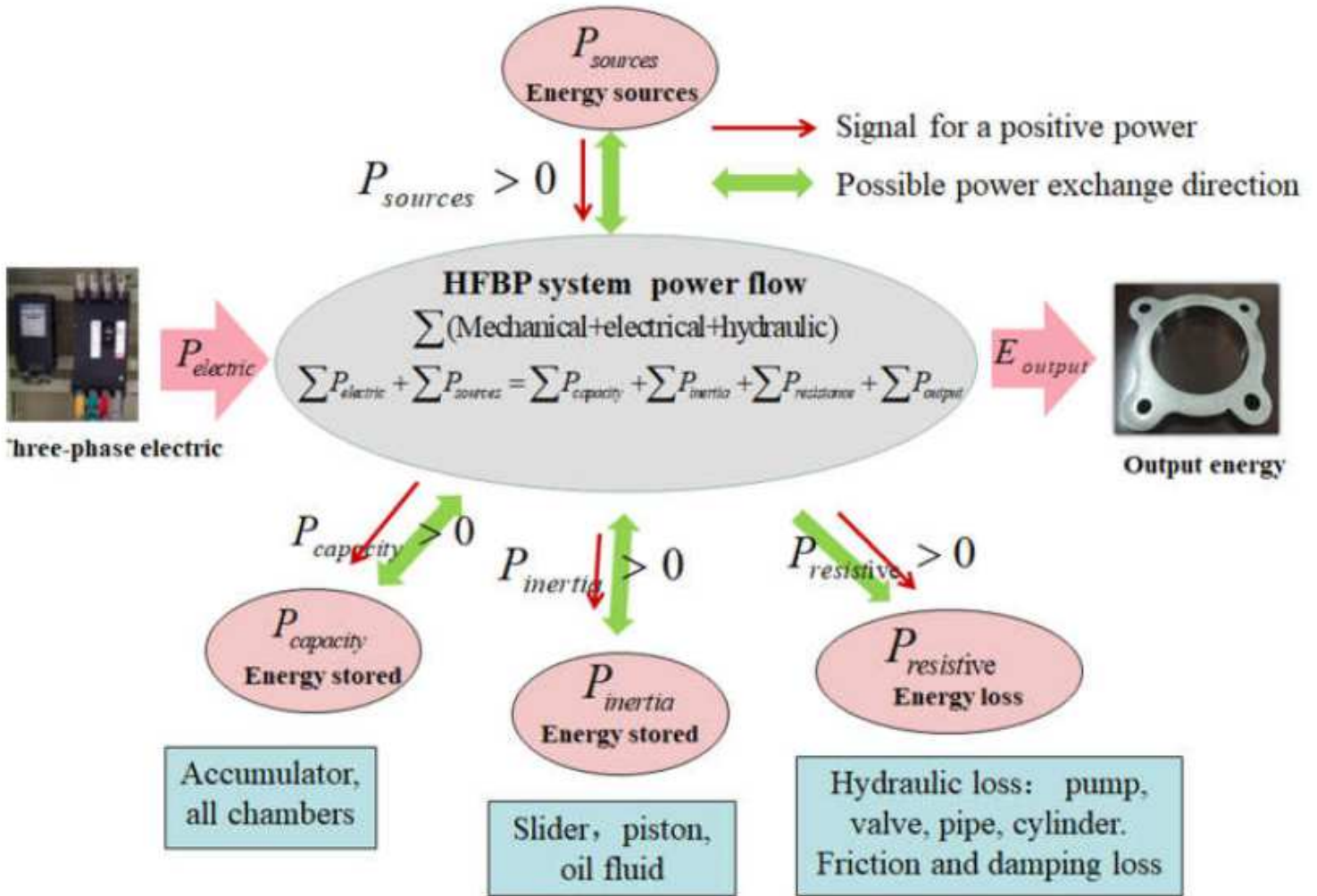


Figure 8

Energy flow chart of hydraulic system.

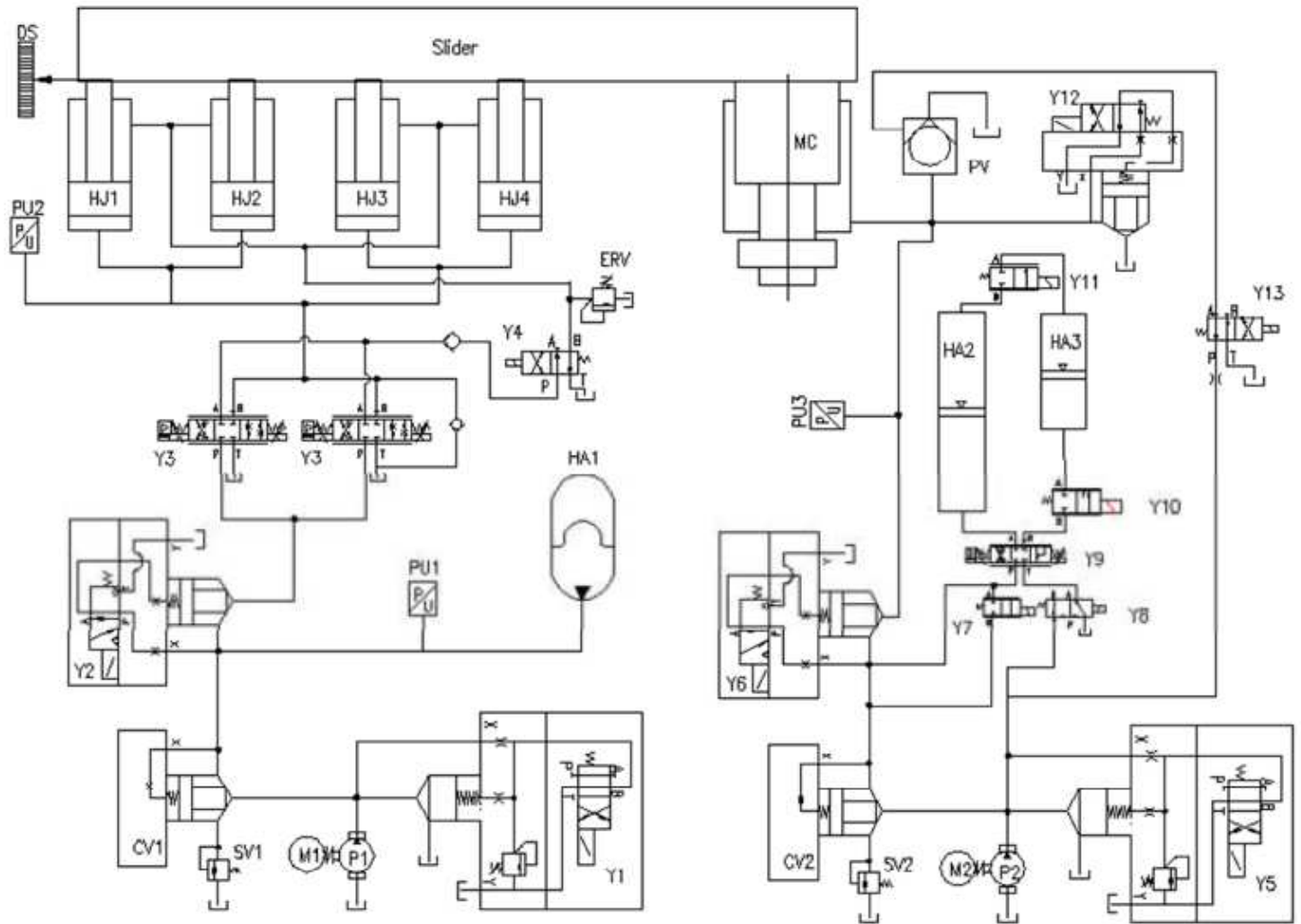


Figure 9

Detailed schematic of 1000 ton hydraulic fineblanking press.

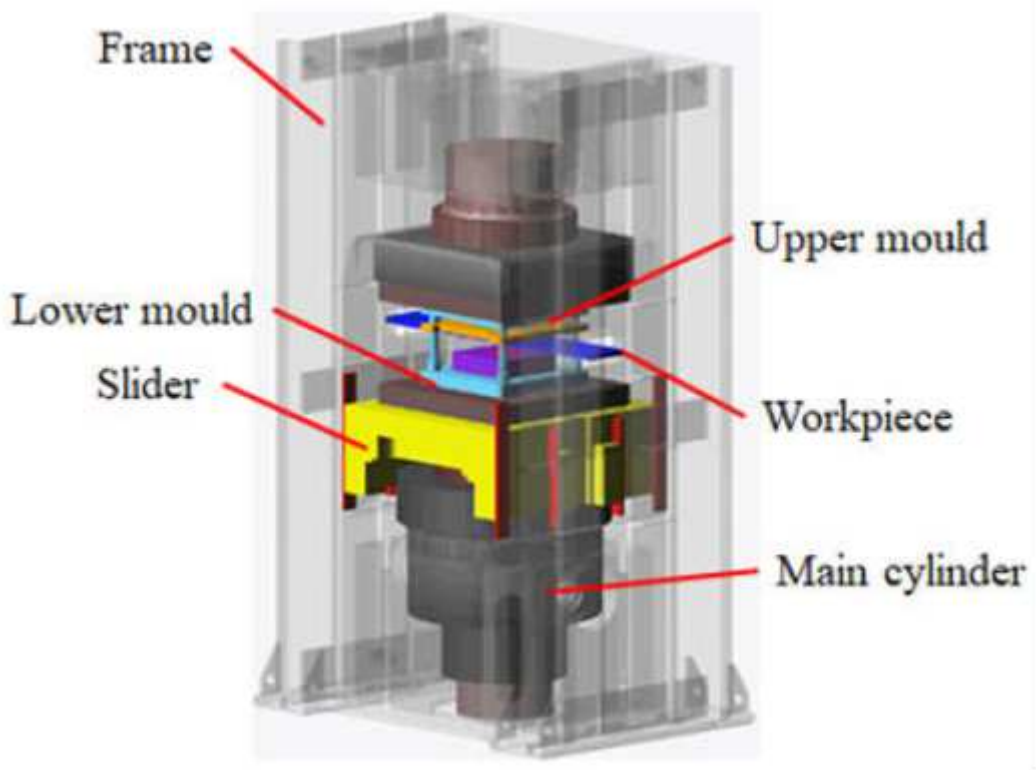


Figure 10

Assembly virtual structure of 1000 ton hydraulic die casting press.

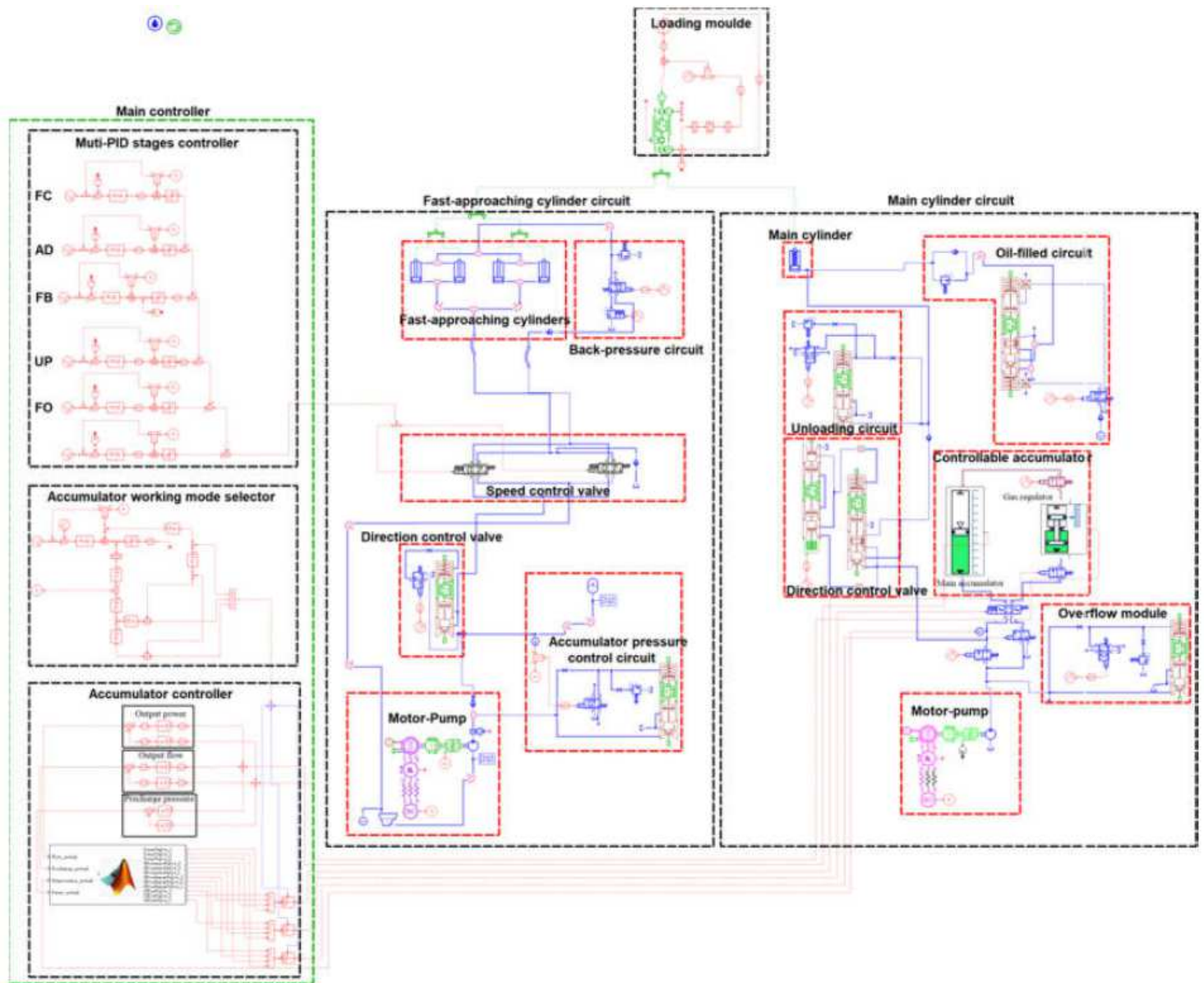


Figure 11

Simulation model of 1000 ton hydraulic fineblanking press

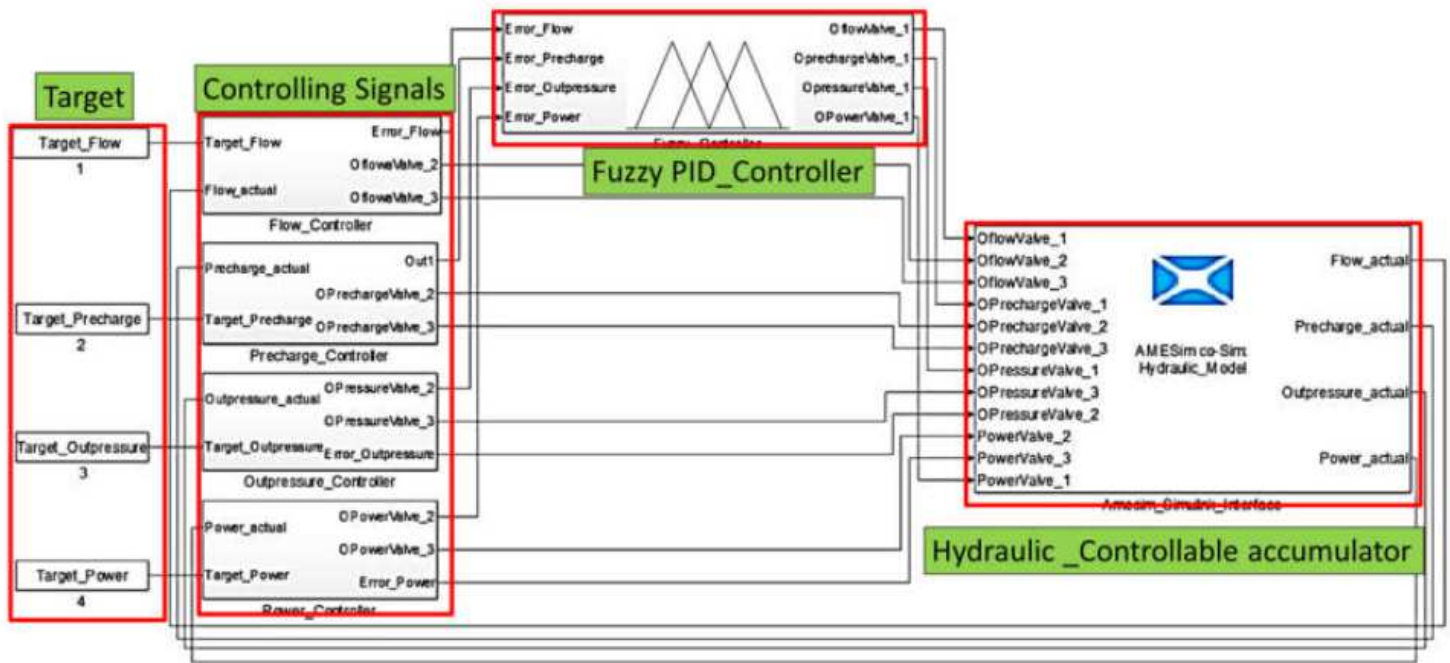


Figure 12

Fuzzy PID controller schematic for the controllable accumulator.

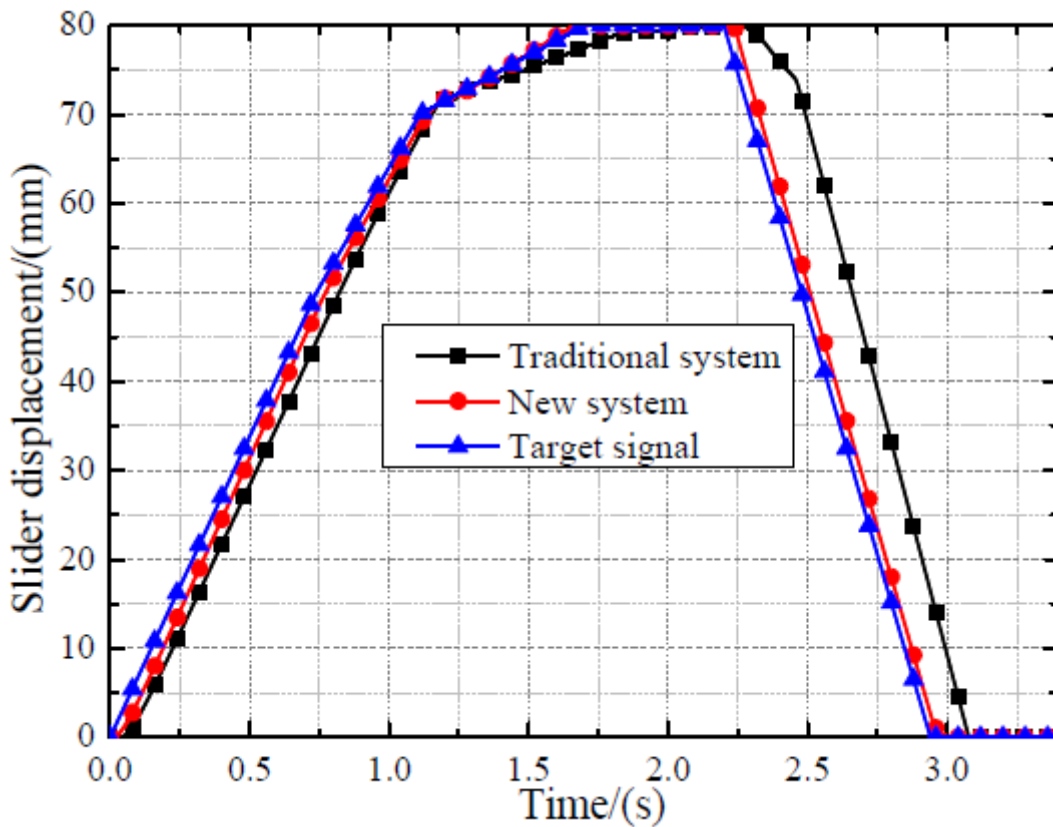


Figure 13

Slider displacement of new system and traditional system.

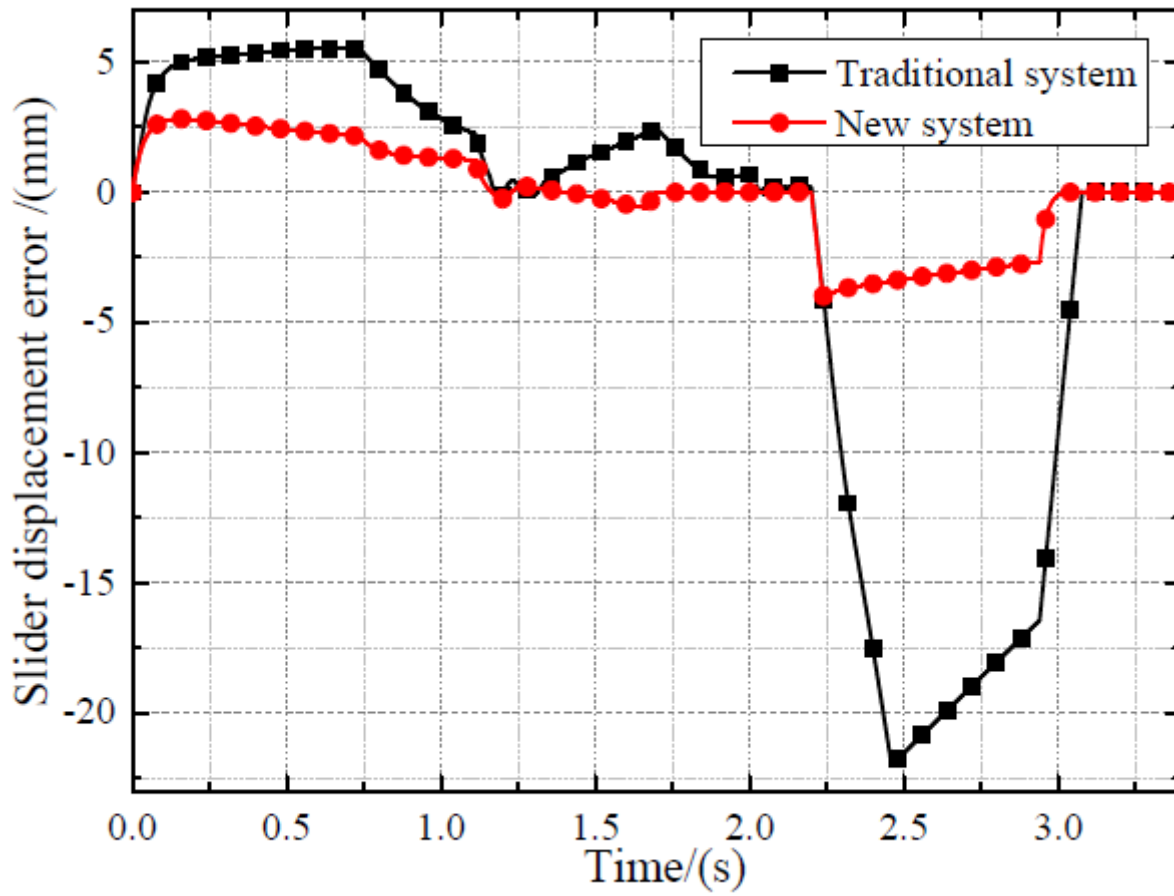


Figure 14

Slider displacement error of new system and traditional system.

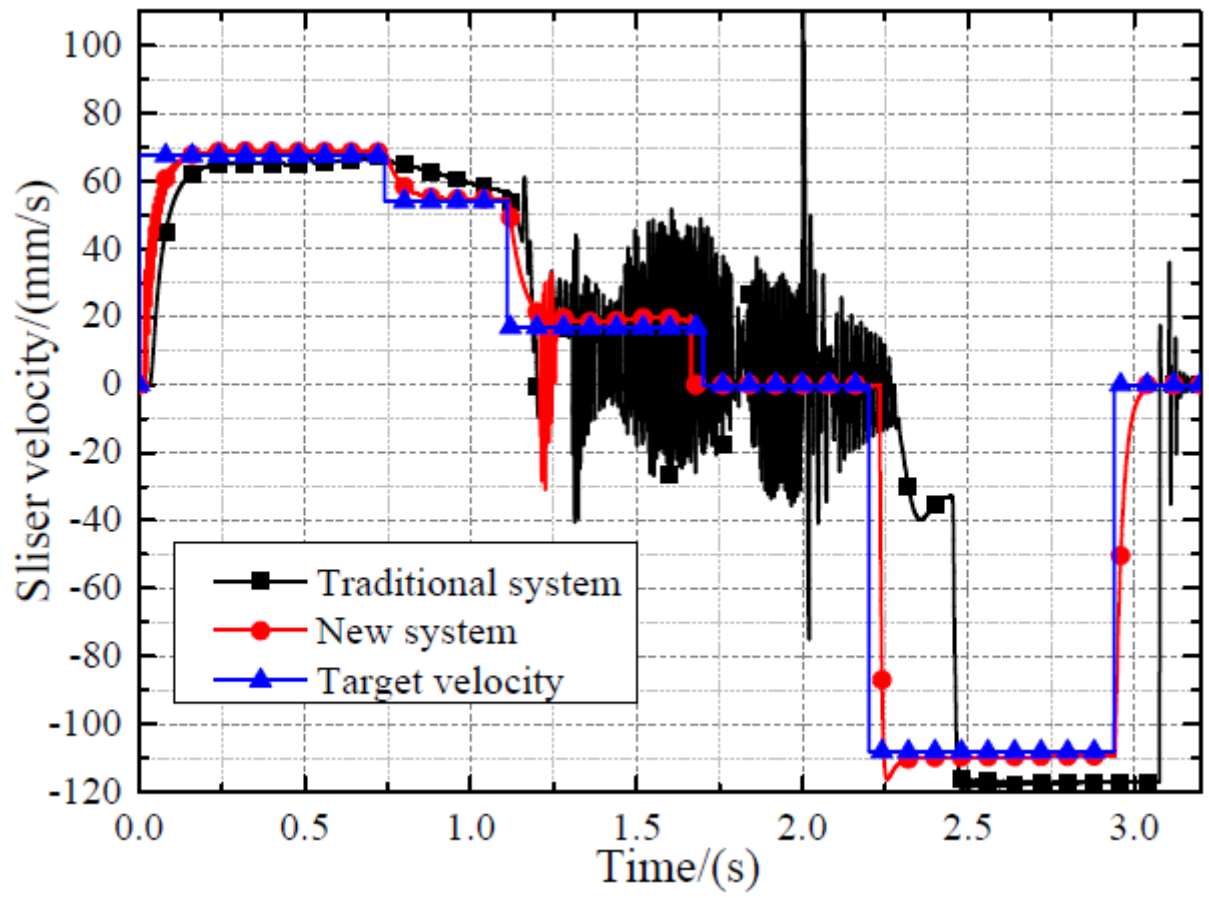


Figure 15

Slider velocity of new system, traditional system and target signal.

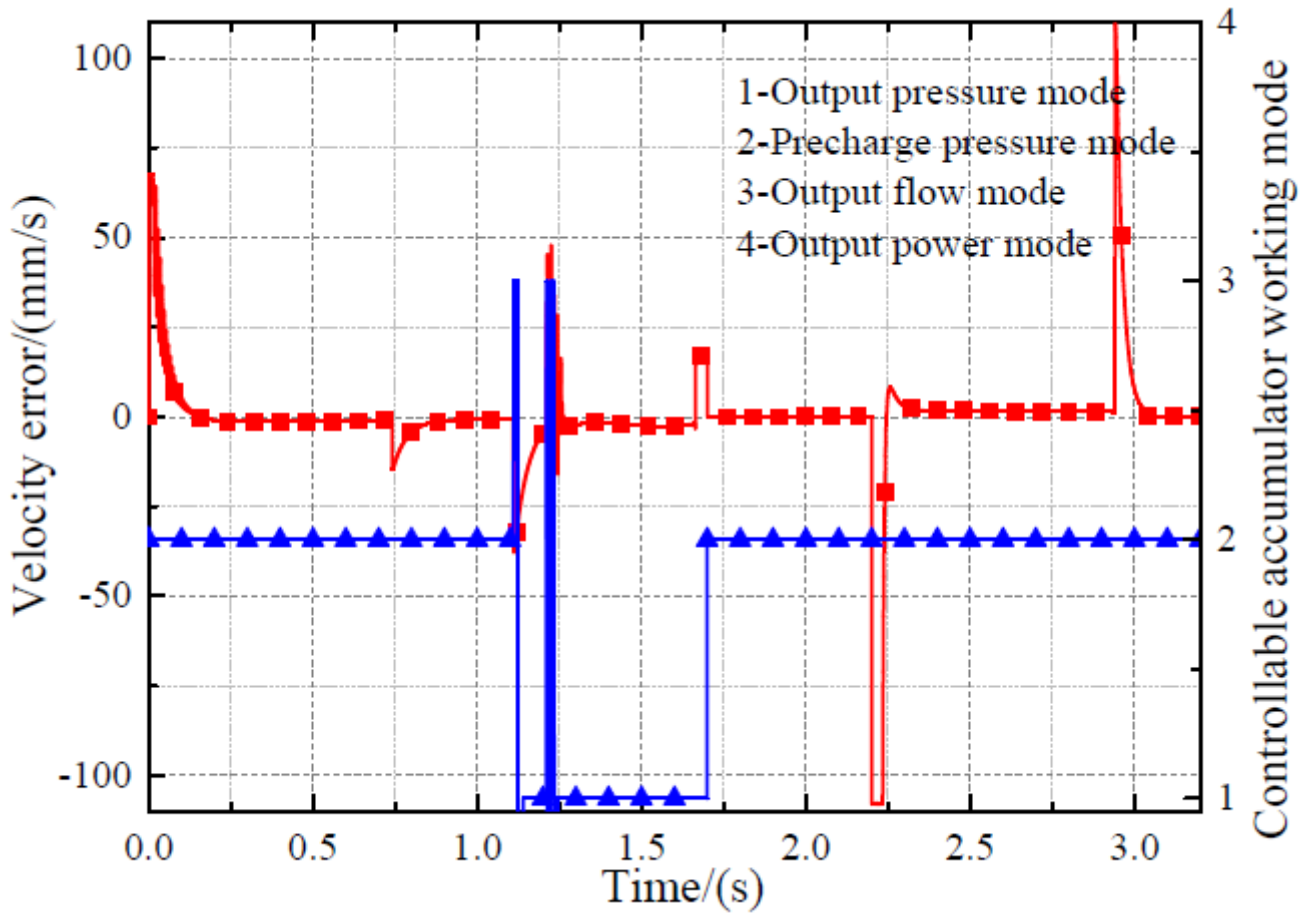


Figure 16

Relationship between the velocity error and the working mode of controllable accumulator.

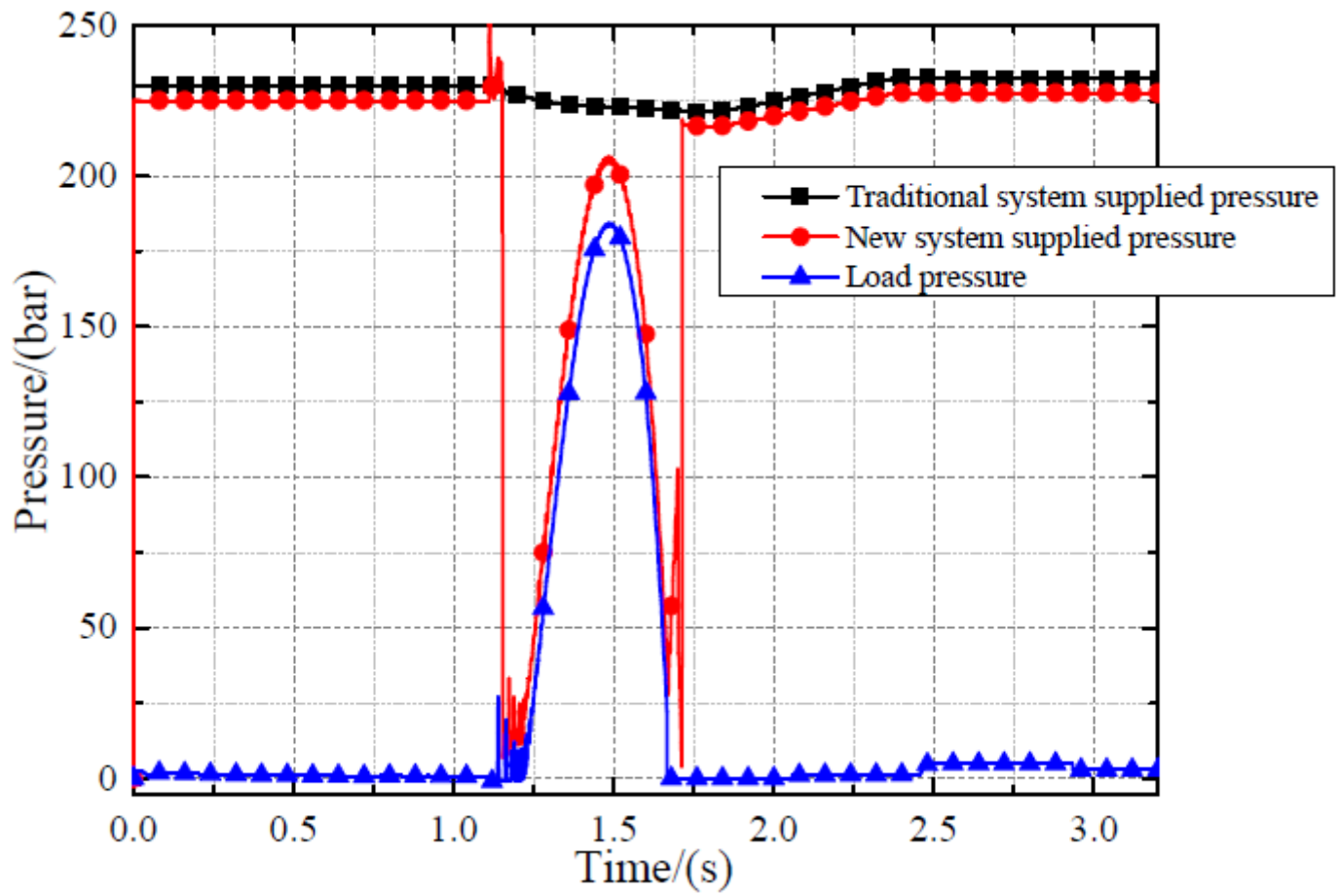


Figure 17

Load pressure and the supplied pressure of traditional system and the new system.

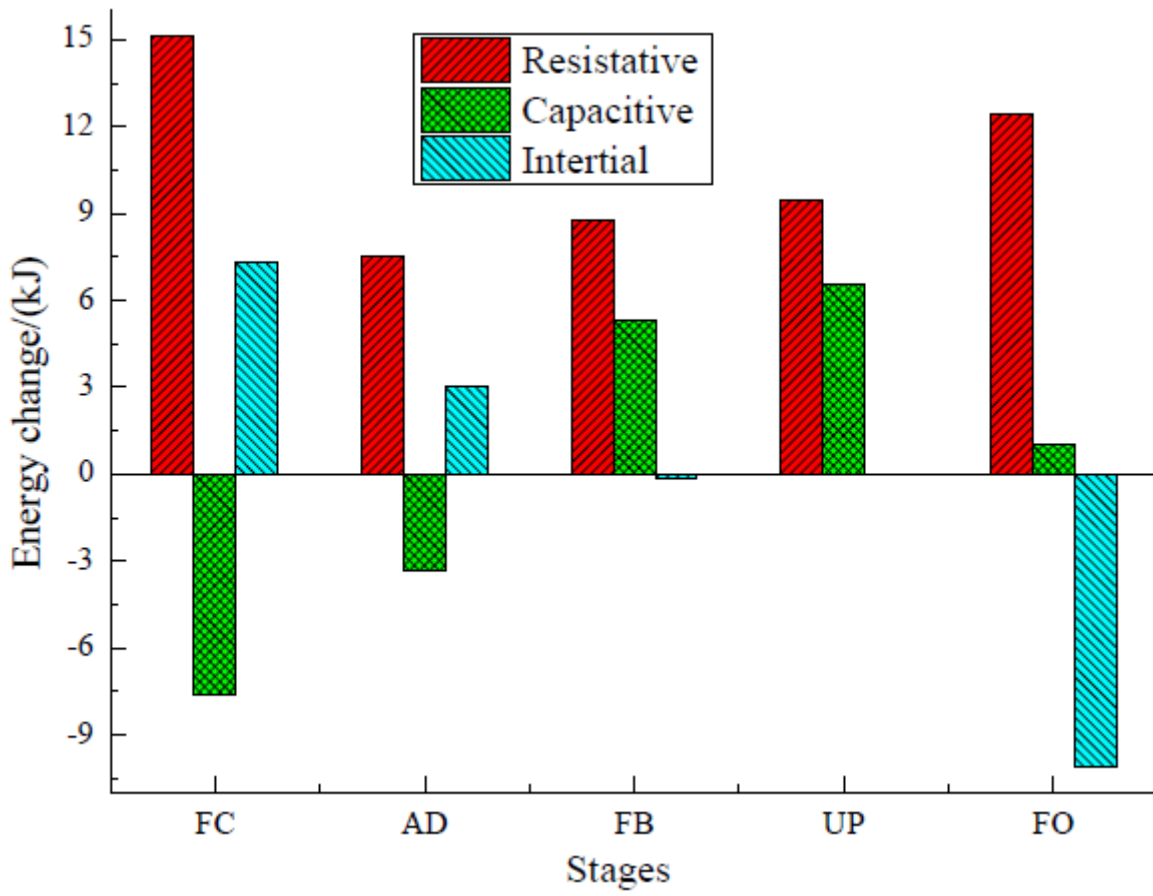


Figure 18

Energy change of resistive, capacitive and inertial energy of fast cylinder circuit.

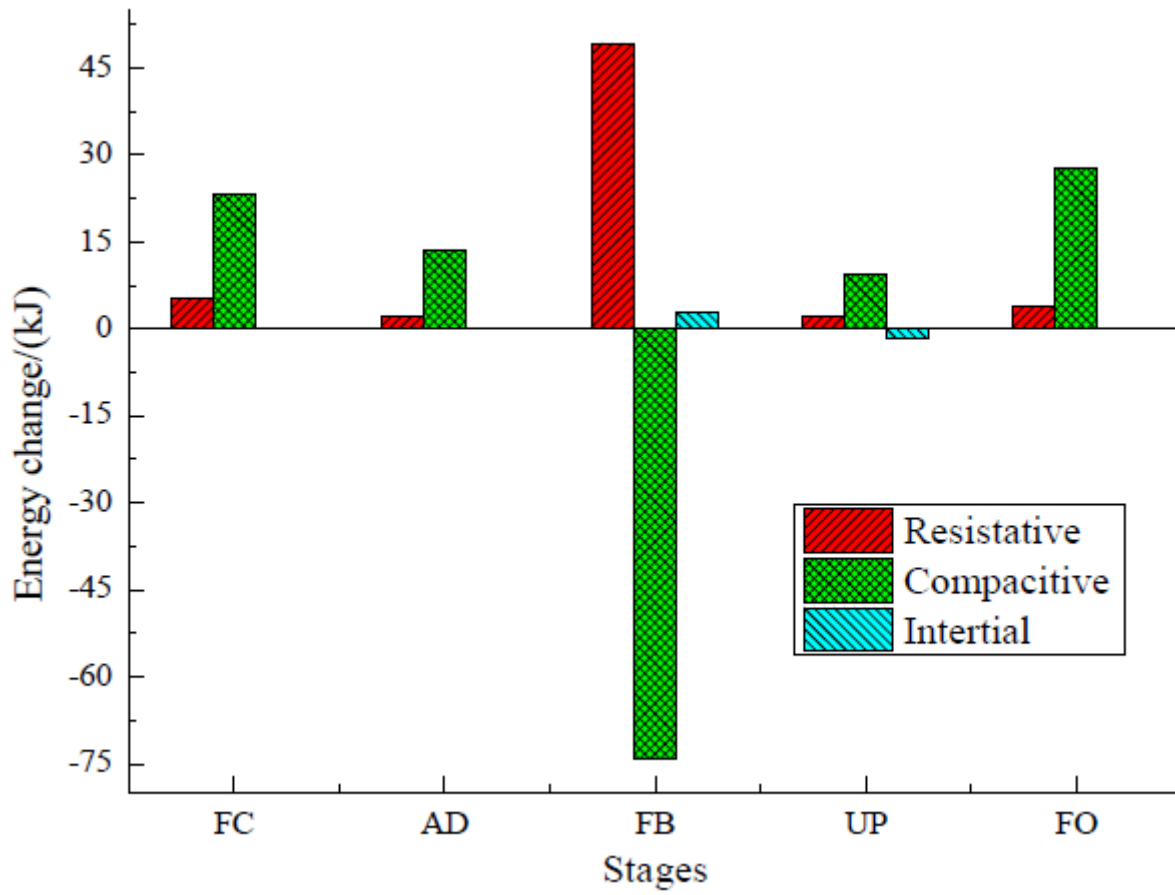


Figure 19

Energy change of resistive, capacitive and inertial energy of main cylinder circuit.

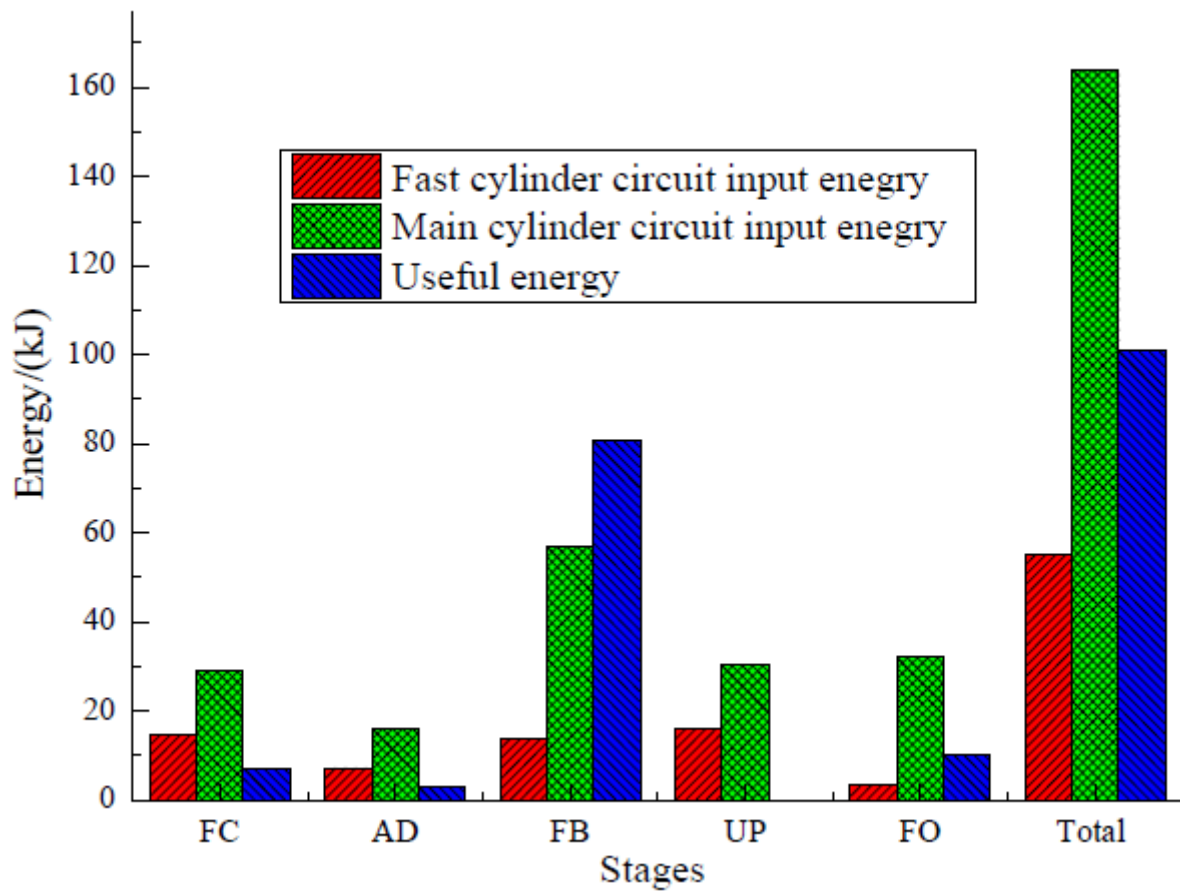


Figure 20

Energy input and useful energy of each stage in new system.

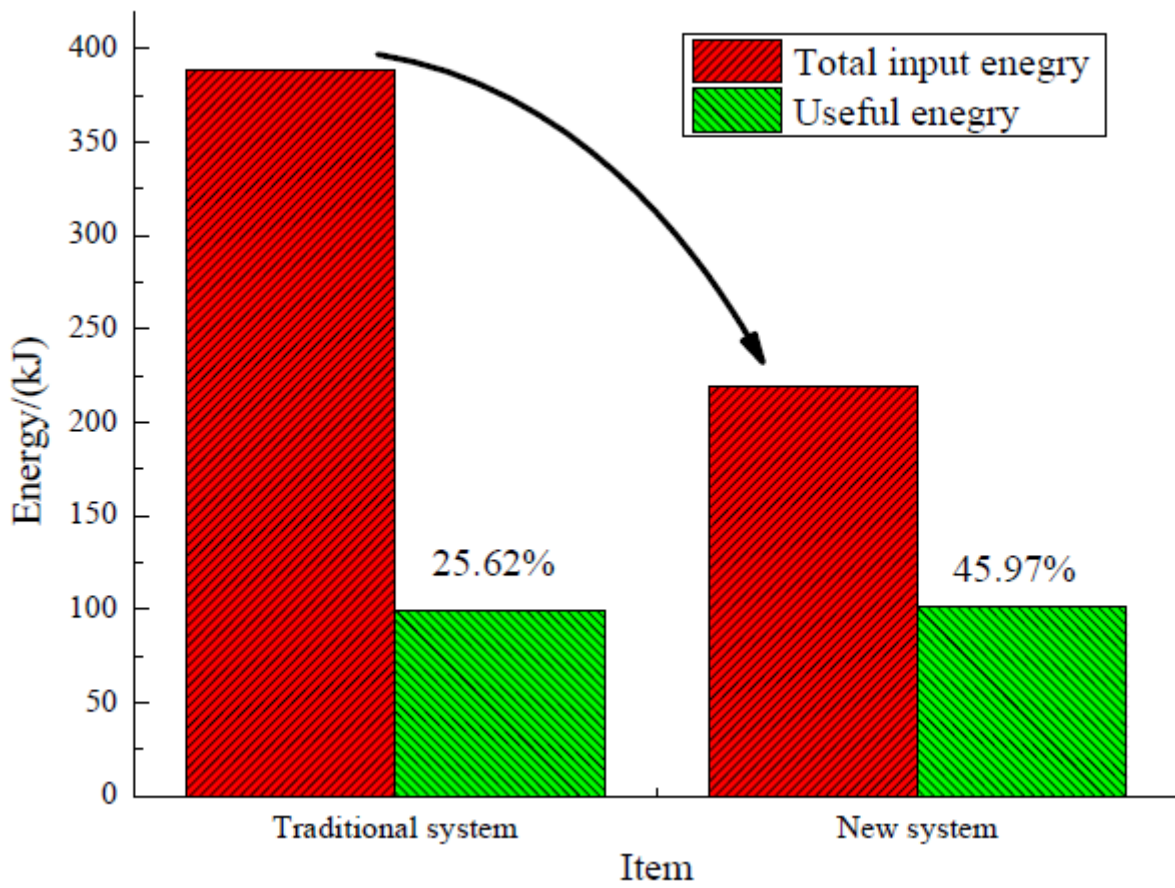


Figure 21

Total input energy and useful energy efficiency of new system and traditional system.